Advancing Flood Detection and Mapping: A Review of Earth Observation Services, 3D Data Integration, and AI-Based Techniques

remote sensing

MDPI

Review

Advancing Flood Detection and Mapping: A Review of Earth Observation Services, 3D Data Integration, and AI-Based Techniques

Tommaso Destefanis [1,2], Sona Guliyeva [2], Piero Boccardo [2,*] and Vanina Fissore [3]

[1] Department of Civil, Building and Environmental Engineering (DICEA), Sapienza Università di Roma, Via Eudossiana, 18, 00184 Rome, Italy; tommaso.destefanis@uniroma1.it
[2] SDG11lab, Interuniversity Department of Regional and Urban Studies and Planning (DIST), Politecnico di Torino, Viale Pier Andrea Mattioli, 39, 10125 Torino, Italy; sona.guliyeva@polito.it
[3] ITHACA S.r.l., 10138 Torino, Italy; vanina.fissore@ithaca.earth
* Correspondence: piero.boccardo@polito.it

Abstract

Floods are among the most frequent and damaging hazards worldwide, with impacts intensified by climate change and rapid urban growth. This review analyzes how satellite-based Earth Observation (EO) technologies are evolving to meet operational needs in flood detection and water depth estimation, with a focus on the Copernicus Emergency Management Service (CEMS) as a mature and widely adopted European framework. We compare the capabilities of conventional EO datasets—optical and Synthetic Aperture Radar (SAR)—with 3D geospatial datasets such as high-resolution Digital Elevation Models (DEMs) and Light Detection and Ranging (LiDAR). While 2D EO imagery is essential for rapid surface water mapping, 3D datasets add volumetric context, enabling improved flood depth estimation and urban impact assessment. LiDAR, in particular, can capture microtopography between high-rise structures, but its operational use is constrained by cost, data availability, and update frequency. We also review how artificial intelligence (AI), including machine learning and deep learning, is enhancing automation, generalization, and near-real-time processing in flood mapping. Persistent gaps remain in model transferability, uncertainty quantification, and the integration of scarce high-resolution topographic data. We conclude by outlining a roadmap towards hybrid frameworks that combine EO observations, 3D datasets, and physics-informed AI, bridging the gap between current technological capabilities and the demands of real-world emergency management.

Keywords: Earth Observation; flood mapping; 3D datasets; LiDAR; Copernicus EMS; artificial intelligence; SAR; DEM; water depth estimation

Academic Editor: Fumio Yamazaki

Received: 29 July 2025
Revised: 20 August 2025
Accepted: 21 August 2025
Published: 25 August 2025

Citation: Destefanis, T.; Guliyeva, S.; Boccardo, P.; Fissore, V. Advancing Flood Detection and Mapping: A Review of Earth Observation Services, 3D Data Integration, and AI-Based Techniques. *Remote Sens.* **2025**, *17*, 2943. https://doi.org/10.3390/rs17172943

1. Introduction

Floods are the most frequent and economically damaging disasters worldwide, impacting infrastructure, agriculture, and urban systems such as transportation and drainage networks [1]. With climate change and urban expansion intensifying flood frequency and severity, rapid flood detection and mapping have become critical for preparedness, emergency response, and long-term mitigation [2].

In disaster response, flood emergency mapping provides near-real-time spatial intelligence on extent and severity, supporting evacuation planning, resource allocation, and recovery [3]. According to official World Health Organization (WHO) statistics reported

by Liu et al. [1], floods account for most natural disasters over the past decade and are increasing in frequency and intensity. This trend, linked to more extreme precipitation under climate change, underscores the need for timely, accurate, and operational flood monitoring—the focus of this review on Earth Observation (EO) and 3D data integration.

This review therefore emphasizes operational EO services and geospatial products that directly support emergency mapping. EO technologies now allow flood monitoring at local to global scales. Synthetic Aperture Radar (SAR) is indispensable for all-weather acquisition [4–6], while optical imagery, despite atmospheric constraints, adds information on vegetation, surface conditions, and land use. When integrated, SAR and optical data provide complementary perspectives [7]. Multi-source fusion with meteorological inputs, hydrological simulations, terrain models, and crowdsourced observations has further improved flood mapping speed and accuracy [4,5,8].

Challenges persist in dense vegetation, urban areas, or low-relief floodplains, where extent detection is less reliable. Moreover, most operational EO systems deliver only 2D flood maps, without volumetric attributes such as water depth or gradients. This review therefore examines the integration of 3D datasets (DEMs, LiDAR, photogrammetry, stereo DEMs, InSAR) with AI-based methods (CNNs, RFs, hybrid physics-informed approaches) to enhance depth estimation and mapping fidelity.

The guiding research question is: How can the integration of 3D geospatial datasets and AI-based techniques improve the accuracy, automation, and real-time performance of satellite-based flood detection and depth estimation, especially in complex terrains? The rationale is three-fold: (i) current methods face sensor and DEM limitations, especially in urban/vegetated areas; (ii) hybrid AI and 3D integration are emerging trends; (iii) operational needs require balancing speed and accuracy for disaster response. To address this, we conducted a narrative review with operational synthesis, based on a structured search (Scopus, Web of Science, Google Scholar, 2015–2025) using keywords such as “flood mapping”, “flood depth estimation”, “LiDAR flood”, “3D flood mapping”, and “machine learning flood”, complemented by operational reports and reference snowballing. Studies were included if they met the following criteria: (i) applied EO data for flood mapping or depth estimation, (ii) provided quantitative or operational results, and (iii) described datasets and methods in sufficient detail. This paper is organized as follows:

- overview of operational services delivering flood products;
- analysis of the Copernicus Rapid Mapping Service in real-world floods;
- review of geospatial datasets for emergency mapping;
- assessment of the added value of 3D datasets for depth estimation and urban im-pacts;
- exploration of AI-based methods to enhance automation, generalization, and real-time performance

2. Operational Earth Observation Services for Flood Monitoring

Among the many initiatives providing EO-based flood information, the Copernicus Emergency Management Service (CEMS) represents the most mature and operationally consolidated framework in Europe, with products routinely delivered to civil protection and humanitarian responders. While several international platforms exist, such as the Dartmouth Flood Observatory or regional services, their availability, continuity, and validation protocols are often heterogeneous. In contrast, CEMS offers a systematic, institutionalized service with standardized workflows and traceable quality assurance, making it a benchmark for operational flood mapping. For this reason, this review prioritizes CEMS and its Rapid Mapping component as a central case study. This section reviews key global and regional EO-based platforms, with particular attention to their operational frameworks, latency, accessibility, and suitability for disaster response.

2.1. Global and Regional EO Platforms for Emergency Flood Mapping

The operationalization of EO technologies has led to a diverse ecosystem of flood monitoring platforms, ranging from legacy institutional systems like Copernicus EMS [8] and NASA GFMS [9] to emerging AI-based services. This subsection synthesizes key global and regional EO-based platforms, focusing on their operational models, accessibility, latency, and relevance in flood response.

Copernicus Emergency Management Service (CEMS) is a flagship European program that delivers both on-demand flood mapping (Rapid Mapping) and continuous global monitoring (Global Flood Monitoring—GFM) [8]. Rapid Mapping is activated by authorized users and provides GIS-ready, vector-based maps within hours of satellite acquisition. These outputs are based on rapid satellite tasking coordinated by the European Response Coordination Centre and Joint Research Centre [10]. During the 2023 Italy floods, the service delivered an initial SAR-derived map within 18 h, followed by regular updates. Similarly, in the 2021 Western Europe floods, CEMS produced 27 high-resolution maps in the first 72 h, supporting field coordination [11]. After the emergency phase, CEMS offers Risk and Recovery Mapping, which includes detailed classifications and multi-temporal analyses [12]. The GFM component provides near-real-time, fully automated global flood maps based on Sentinel-1 SAR data, updated every 6 h. For example, during the 2022 Pakistan floods, GFM achieved a Critical Success Index (CSI) of ~0.8, reliably tracking over 30,000 km^2 of inundation over six weeks [13,14].

While Copernicus EMS remains the most widely used operational service in Europe, NASA's Global Flood Monitoring System (GFMS) offers a complementary, globally scalable approach based on hydrological modeling. GFMS, developed by the University of Maryland, is a semi-operational, model-based platform using satellite precipitation data to simulate runoff and river discharge globally [15,16]. Updated every 3 h, it provides near-real-time and 5-day forecasts of flood extent, streamflow, and water depth at ~1 km resolution [17]. Its strength lies in global coverage and predictive capabilities, especially in data-sparse regions. The World Food Programme (WFP) routinely uses GFMS for early flood alerts, as seen during the 2015 Malawi floods [18]. Validation studies have reported a >90% detection probability (POD) for large events, though false alarm rates reached ~65%, especially for short-lived floods, due to model limitations with dams and spatial resolution [19].

The Dartmouth Flood Observatory (DFO) provides both a historical flood archive and near-real-time mapping. Its MODIS-based products detect large-area inundation (250 m resolution) using composite imagery over 2–3 days, while the River Watch system uses passive microwave sensors for twice-daily updates [20]. During the 2022 Pakistan floods, DFO mapped up to 56,000 km^2 of inundation [21]. Its Web Map Service is widely used by the UN and humanitarian agencies, though urban and vegetated areas remain challenging due to resolution limits [22].

The CEOS Flood Pilot (2014–2017) was a multi-agency demonstration led by the Committee on Earth Observation Satellites [15,23,24]. It demonstrated the feasibility of multi-sensor, multi-agency flood dashboards, tested during floods in Sri Lanka [25], and left a legacy of methodological guidelines that informed systems like Copernicus GFM. One of its key goals was a Global Flood Dashboard that would serve as a "one-stop shop" for various satellite flood maps and forecasts [26]. However, its activity ceased after 2017 due to its non-operational nature and dependence on temporary funding [15].

Sentinel Asia, managed by JAXA, supports Asia–Pacific flood mapping via emergency activations. For example, during Cyclone Tauktae (May 2021), it delivered SAR-based inundation maps for Gujarat within ~48 h. While valuable for regional coordination, the system is semi-manual and variable in latency and product quality [27–29].

In recent years, artificial intelligence has increasingly supplemented traditional EO approaches. Google Flood Hub provides AI-driven flood forecasts with up to 7 days of lead time, operational in over 100 countries and reaching approximately 700 million people [30,31]. The system improved evacuation planning during the 2022 Indus Basin floods in Pakistan by offering timely warnings [32]. Microsoft's AI for Good Lab focuses on near-automatic flood mapping through open-source U-Net models trained on Sentinel-1 SAR data, accessible via the Planetary Computer [33]. Microsoft also collaborates with ICIMOD to monitor glacial lakes in the Himalayan region, to identify potential glacial lake outburst flood hazards using AI-assisted EO and hydrodynamic modeling.

The reviewed platforms differ significantly in latency, resolution, accessibility, and analytical approach. Institutional systems like Copernicus EMS [34] and GFMS [9] offer mature frameworks, while academic (DFO) and regional (Sentinel Asia) services provide complementary capacities. AI-driven platforms [33,35] are closing gaps in forecast lead time and automation. These comparisons are summarized in Table 1, which contrasts the platforms' core characteristics and operational trade-offs.

Table 1. Summary of operational Earth Observation services for flood mapping. Temporal coverage varies across platforms, with CEMS active since 2012, Dartmouth Flood Observatory since the mid-1980s (with limited updates after 2020), UNOSAT since 2003, and NASA GFMS since 2011.

Platform/Initiative	Update Frequency/Latency	Access Model	RS Images	Primary Use Case	Key Strengths	Limitations
Copernicus EMS (Rapid Mapping)	~12 h from satellite acquisition (typically <24 h total)	On-demand via EU Civil Protection (authorized users only)	Sentinel-1 SAR, Sentinel-2 optical, Copernicus Contributing Missions (VHR/HR optical and SAR)	Emergency rapid mapping (disaster response)	High-resolution, timely vector maps; standardized outputs	Activation restricted to authorized users in Europe/partners
Copernicus EMS (GFM)	Every 6 h after satellite overpass	Fully automated, open access via web viewer and API	Sentinel-1 SAR	Continuous global flood monitoring	High-frequency SAR-based global coverage; low latency	Limited to surface water from Sentinel-1 SAR; no depth estimates
NASA GFMS	Every 3 h (real-time) + 5-day forecasts	Open access via website and FTP/API	Hydrological models based on satellite precipitation data (e.g., TRMM, GPM)	Global flood forecasting and early warning	Model-driven forecasts; useful in data-sparse regions	Coarse resolution (~1 km); high false alarm rate for short floods
Dartmouth Flood Observatory (DFO)	~1–3 days (MODIS composite); twice-daily (microwave River Watch)	Open access via WMS and downloads	MODIS optical; passive microwave sensors such as AMSR-E, AMSR2	Historical archive and near real-time flood mapping	Long archive; global scope; supports humanitarian users	Low resolution (250 m MODIS); limited urban/vegetated detection
Sentinel Asia	~24–72 h post-activation	Semi-manual activation by member agencies	Multi-mission optical and SAR imagery from contributing satellites	Asia–Pacific regional emergency support	Regional collaboration; SAR under cloud cover	Latency varies; quality varies across Data Analysis Nodes (DANs)
CEOS Flood Pilot	Event-based (2014–2017)	Demonstration only; ceased in 2017	Multi-sensor use (SAR + optical) from partner missions	Methodology testing; global coordination	Inter-agency data integration; dashboard prototypes	Not operational; no sustained updates or data services
Google Flood Hub	Up to 7 days lead time (forecasts)	Open via Flood Hub, Google Search, Maps, APIs	Not specified; modeling system with hydrological and rainfall data, non-public sources	Public alerts and evacuation decision support	Forecasts in +100 countries; long lead time; widely used	Model internals not public; lacks back-end transparency
Microsoft AI for Good	On-demand model execution	Open-source models via Planetary Computer API	Sentinel-1 SAR	SAR-based AI flood detection	Fast SAR-based mapping; replicable; open AI tools	Requires coding skills and infrastructure; limited validation

2.2. Structure and Implementation of the Copernicus Emergency Management Service

CEMS is a core service of the Copernicus program, providing vital geospatial information to support all phases of the emergency and disaster management cycle. Since 2012, CEMS has operated 24/7, delivering EO-based mapping and early-warning products without interruption [36]. It has been activated more than 1000 times, providing support to all EU Member States and over 120 countries worldwide, and has become an essential tool for emergency managers. The focus on CEMS Rapid Mapping is driven by its role as the most mature and operational satellite-based emergency mapping service in Europe, with a fully standardized workflow from data acquisition to product delivery. The service leverages multi-sensor imagery, including Sentinel-1, Sentinel-2, and Copernicus Contributing Missions, to ensure rapid coverage even under cloud or night conditions. Its long track record and proven reliability make it a representative case for examining the operational integration of 3D datasets into flood mapping.

CEMS consists of two main components: an Early Warning and Monitoring component for hazard forecasting, and an **On-demand Mapping** component for rapid geospatial mapping in crises [37]. Early warning and monitoring services continuously produce forecasts and alerts for floods (like with EFAS and GloFAS), fires (EFFIS), and droughts (EDO/GDO) by combining satellite data, in situ measurements, and numerical models [38]. On-demand mapping (also referred to as CEMS Mapping) provides fast geospatial analysis and mapping during and after events, based on high-resolution satellite imagery [38,39]. The service has continuously refined its methods and products through technological upgrades and user feedback from annual workshops and close collaboration with stakeholders like the European Commission's Emergency Response Coordination Centre (ERCC) [38]. A dedicated validation program independently checks a sample of mapping products for accuracy and usefulness [40].

CEMS Mapping can only be triggered by Authorized Users, primarily national focal points of EU Member States [41]. Activations are evaluated by the ERCC within 3–4 h to ensure alignment with the EU emergency framework [42]. CEMS teams then rapidly acquire satellite imagery, and thanks to a standardized workflow, initial products can be generated within just a few hours of image reception. In practice, a full rapid mapping cycle usually spans from a few hours up to a day or two, depending on data availability and urgency. Final products are freely available via the EMS portal, unless they are deemed sensitive and are delivered through a restricted channel [40,43].

The On-Demand Mapping service is divided into two complementary modules tailored to different disaster management needs [40]:

- Rapid Mapping (RM): an emergency "rush mode" service active 24/7, which provides geospatial information within hours or days of a disaster to support immediate response. It focuses on quickly mapping the event extent and assessing damage.
- Risk and Recovery Mapping (RRM): a "non-rush" service available during working hours. It supports pre- and post-crisis phases such as prevention and long-term recovery. These activations produce more detailed analytical products that can take days or weeks.

Both modules rely on a consortium of service providers to fulfill mapping requests. Service quality is monitored via standardized procedures, and an independent validation team evaluates a subset of maps by comparing them with external reference data to quantify their reliability and usefulness [40]. All Rapid Mapping outputs are provided in standard formats and made available on the public EMS portal. The Rapid Mapping service has a well-defined portfolio of five standard product types [44,45]:

- First Estimate Product (FEP): provides an early, approximate overview of the disaster, helping to prioritize areas for detailed mapping [46].
- Delineation Maps (DEL): define the spatial extent of the event using post-event imagery, crucial for identifying impacted areas [47].
- Grading Maps: classify damage severity to assets.
- Reference Map (REF): a pre-event map that compiles baseline information, useful for impact assessment in regions lacking recent geospatial data.
- Situational Reporting (SR): a live, online report that summarizes the situation using CEMS products and external sources.

For detection, Copernicus EMS combines manual, automated, and hybrid image analysis methods to balance speed and accuracy. Manual interpretation by experts is used in complex contexts, while automatic routines like thresholding or pixel-based change detection are applied when conditions allow [10,48,49]. The Copernicus Emergency Management Service (CEMS) – Rapid Mapping Portfolio for Emergency Response. is shown in Figure 1.

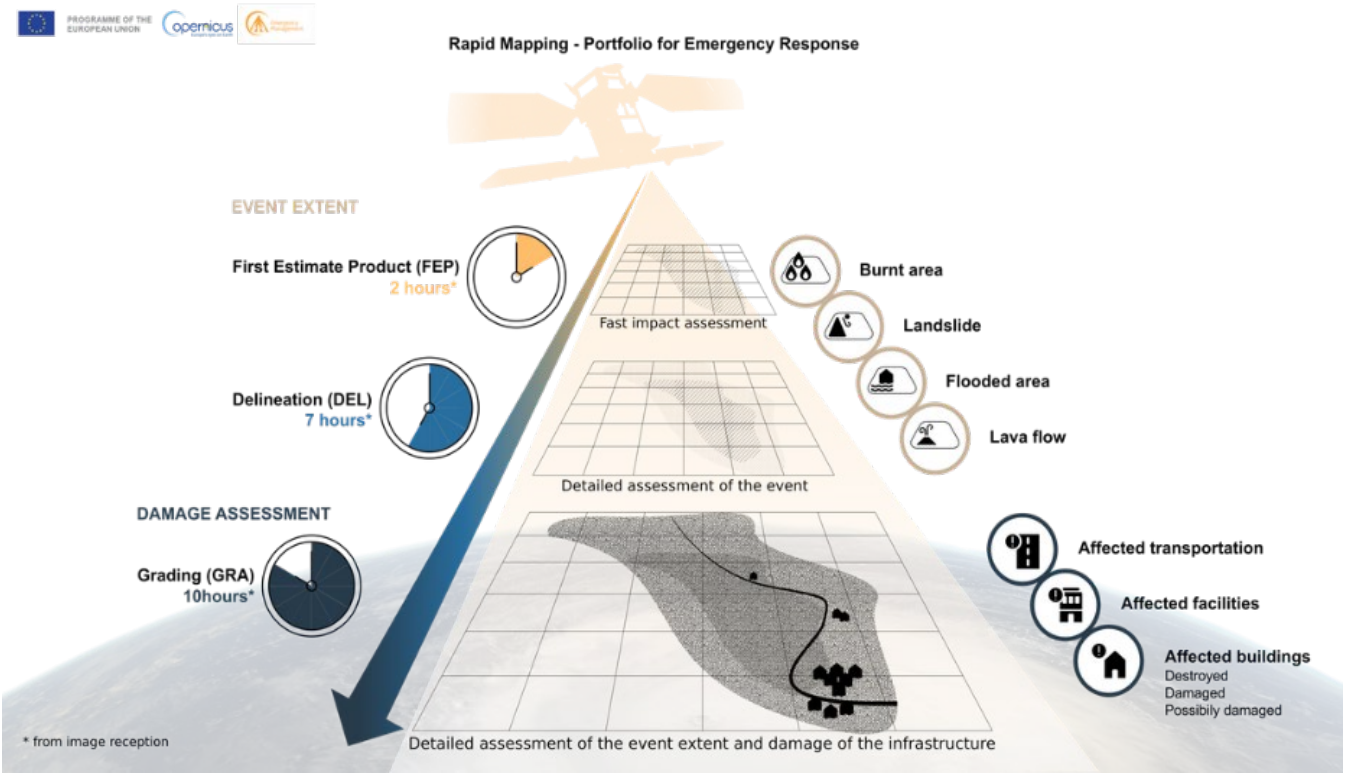

Figure 1. Copernicus Emergency Management Service (CEMS)—Rapid Mapping Portfolio for Emergency Response. Contains modified Copernicus Sentinel data (2023–2024), processed by the European Union, Copernicus Emergency Management Service, © European Union, 2025.

A particular challenge is satellite-based building damage assessment in the immediate aftermath of disasters. Overhead imagery can miss structural failures like internal collapse, and image resolution, sensor angles, and even analyst subjectivity introduce uncertainties. Recognizing that traditional ground-based damage scales, such as the five-grade European Macroseismic Scale EMS-98 for earthquakes, cannot be directly applied, Copernicus EMS developed a simplified grading scheme for its rapid damage maps [50].

The EMS-98's five damage levels are consolidated into three broad classes for satellite mapping: Destroyed, Damaged, and Possibly Damaged. These correspond to heavy destruction, moderate/substantial damage, and slight or uncertain damage, respectively. Two special flags are also used: Not Visible Damage (when no damage is apparent from

the imagery, which does not mean no damage exists on the ground) and Possibly Damaged as an uncertainty flag. Each damage class is defined by observable image features—for example, Destroyed typically means a building's outline is largely obliterated, while Damaged might mean roof or structural changes indicating partial failure. This standardized classification is applied across all disaster types to ensure consistency [51]. It provides first responders with a quick proxy of damage severity on a map, helping to prioritize areas for on-site inspection.

However, CEMS always cautions that these are apparent damage levels from remote sensing—a near-real-time estimation—and not a substitute for detailed ground surveys. This limitation is acknowledged in EMS documentation, which emphasizes the maps' role as "situational awareness" rather than "ground truth" [48]. Users must be aware of the inherent uncertainties and use the maps as guidance for further investigation rather than as a definitive truth. Despite these caveats, the rapid damage maps are extremely valuable for situational awareness, delivering timely information to emergency managers when they need it most.

2.3. Integration of EO-Based Flood Products into Decision-Making Processes

Flood extent products from operational EO services are essential tools for emergency responders and civil protection agencies. By clearly delineating inundated areas and identifying affected infrastructure, they enable timely, evidence-based decisions in fast-changing disaster environments [52,53]. These products transform satellite data into actionable intelligence by offering spatially explicit insights on water extent and asset exposure, informing critical decisions across the disaster management cycle. The scientific rigor and timeliness of these products ensure that end-users can trust them for high-stakes decisions [54]. For instance, CEMS provides authorized agencies with geo-spatial flood information that can be used directly or integrated into geographic information systems to support emergency decision-making [8,54]. Empirical studies confirm that real-time satellite flood mapping enhances coordination, optimizes resource deployment, and supports safety planning during crises [55]. In sum, EO flood maps offer rapid situational awareness, enabling emergency managers to plan and coordinate relief efforts efficiently [54,56,57].

Once the immediate threat subsides, flood maps continue to support a broad range of recovery and planning functions. Beyond the immediate response, policymakers and urban planners utilize flood maps for long-term risk reduction. Detailed maps enable quantitative assessment of damages to communities and critical infrastructure, forming the basis for funding allocation and reconstruction planning. Archival EO data support the calibration and refinement of inundation models [58]. Under the EU Floods Directive, Member States are required to produce flood hazard and risk maps, and EO-derived products provide essential input to this process [59,60]. Additionally, stakeholders such as the insurance industry refer to validated flood maps when estimating losses or setting premiums. Operational flood maps thus find applications from the height of an emergency through to post-event analysis and mitigation planning, contributing to building more resilient communities [61].

In conclusion, flood maps from operational EO services have evolved into critical decision-support assets for a broad spectrum of users. Whether it is a civil protection officer planning an evacuation or an urban planner designing resilient communities, these maps provide the scientific evidence to make informed choices. By delivering where, when, and the severity of flooding in a clear geospatial format, they bridge the gap between satellite observations and ground action. Furthermore, continual improvements since 2020, including AI-enhanced analytics and interactive dashboards, have increased their relevance [62]. As a result, societies are better equipped not only to respond to floods but

also to learn from them, adapt, and reduce future risks, fulfilling the promise of Earth observation in service of disaster resilience [63].

In synthesizing these systems, a trade-off becomes evident. Institutional platforms like Copernicus EMS and NASA GFMS provide validated, high-resolution outputs for coordinated emergency response, while emerging AI-based services like Google Flood Hub rapidly advance forecasting capabilities, particularly in underserved regions. This contrast reflects a broader tension between latency, spatial resolution, and ease of integration into decision-making workflows. High-resolution products from satellite tasking can be delayed, whereas AI-based systems offer longer lead times but may lack spatial detail. As operational needs evolve, there is growing consensus around the value of hybrid frameworks that blend predictive AI models with EO-based observational inputs. Such integration leverages both the robustness of EO data and the temporal foresight of AI-driven forecasts, which will be critical for next-generation platforms.

The comparative analysis of platforms has shown that differences in latency, spatial resolution, and accessibility are closely linked to the type and quality of their input datasets. The ability to deliver timely and accurate flood maps ultimately depends on the availability of suitable satellite data and the robustness of pre- and post-processing workflows. Understanding which datasets are employed is therefore essential to explain operational differences and to identify areas for improvement. The following section will examine in detail the geospatial datasets and processing methods that form the foundation of EO-based flood mapping, highlighting how the selection and integration of different sources directly influence the accuracy and timeliness of the final products.

3. Geospatial Datasets and Processing Foundations for Flood Mapping

The effectiveness of EO-based flood monitoring depends not only on platform capabilities but also on the underlying geospatial datasets and processing methods that convert satellite observations into actionable information. Different data sources—ranging from SAR and optical imagery to DEMs, LiDAR, photogrammetry, and InSAR—provide complementary perspectives on flood dynamics, but also introduce specific limitations in terms of resolution, coverage, and acquisition frequency. These characteristics directly affect whether floods can be mapped in two dimensions (extent) or three dimensions (depth and volume). Ancillary datasets such as crowdsourced observations, hydrological models, and meteorological inputs are increasingly integrated to bridge observational gaps and to improve situational awareness in near-real time.

This section reviews the core geospatial datasets and methodological approaches used in flood emergency mapping, with three guiding questions: (i) what information each dataset contributes to flood detection and depth estimation; (ii) what constraints arise from their spatial, temporal, and thematic resolution; and (iii) how their integration through multi-sensor fusion and AI techniques enhances detection accuracy, spatial resolution, and operational readiness

3.1. Remote Sensing and Ancillary Datasets for Flood Detection

Optical satellite imagery provides intuitive and widely used tools for flood mapping. Multi-spectral sensors such as Sentinel-2, Landsat-8/9, MODIS, and PlanetScope support water detection through indices like NDWI, MNDWI, and NIR/SWIR reflectance thresholds. These datasets are particularly effective under clear-sky conditions, enabling high-resolution mapping of flood extent, vegetation stress, and land cover impacts. Sentinel-2, in particular, is the backbone of many flood extent analyses, including products from Copernicus EMS [64]. During the 2022 Pakistan floods and the 2023 Emilia-Romagna

floods in Italy, optical imagery proved instrumental for post-event mapping and damage assessment [7,12,15,65–68].

However, optical sensors face important constraints. Their reliance on daylight and cloud-free conditions makes them less reliable during peak flood periods, when rapid assessments are most critical [69,70]. Moreover, classification errors may arise in complex environments: for example, studies in the Ebro River Basin showed that dense vegetation can lead to water misclassification, as reflections from wet vegetation distort spectral signals [15].

Synthetic Aperture Radar (SAR) is a cornerstone for flood mapping, as it operates independently of weather and daylight, enabling reliable detection during storms and at night [71]. Several SAR missions contribute to operational flood response: Sentinel-1, widely applied in the Ebro and Po River Basins, provides systematic coverage; ALOS-PALSAR 2 (L-band) enhances detection under vegetation canopies due to its longer wavelengths; and COSMO-SkyMed and RADARSAT-2 supply critical data for near-real-time monitoring [71]. Within Copernicus EMS, SAR—especially Sentinel-1—is the primary dataset for delineation mapping, with proven effectiveness in multiple Rapid Mapping activations [72]. To improve the revisit frequency and pre-event baselines, EMS integrates Sentinel-1 with PlanetScope and SkySat imagery, enabling near-real-time updates and historical comparisons [73,74]. Commercial providers further extend these capabilities: ICEYE delivers building-scale flood extent and depth estimates in near-real time, while Planet Labs supplies high-frequency optical data (3–5 m resolution) for refined flood tracking. During major disasters, both often release imagery under the International Charter on Space and Major Disasters.

Passive microwave and thermal infrared sensors provide complementary information for flood risk forecasting and post-event assessment. Passive microwave missions such as SMAP, SMOS, AMSR-2, and GPM deliver large-scale observations of soil moisture and precipitation that are critical for flood risk anticipation and early warning. Although their spatial resolution is coarse, these datasets are particularly valuable in ungauged basins or data-scarce regions. For example, SMAP soil moisture products have been employed to quantify surface saturation prior to major floods, enhancing risk models and early action protocols. In parallel, thermal infrared sensors (e.g., MODIS TIR, ECOSTRESS) provide indirect flood indicators by detecting surface cooling patterns linked to soil wetness and standing water. Post-event thermal anomalies can help delineate residual inundation zones, particularly when integrated with optical or SAR imagery.

To improve delineation accuracy and enable 3D analysis, flood mapping increasingly integrates Digital Elevation Models (DEMs). High-resolution DEMs from LiDAR [75] or TanDEM-X support floodplain characterization, water depth estimation, and hydrodynamic modeling. Combining SAR-derived flood extent data with elevation data allows depth estimation through methods such as morphological expansion or DEM-difference [76]. A recent framework by Betterle and Salamon (2024) uses DEM-based reasoning to fill sensor gaps and derive floodwater heights from boundary elevations [77].

LiDAR is especially valuable in dense urban areas, where its ability to capture fine-scale topography enhances both flood extent and depth modeling. Airborne surveys conducted post-event can map high-water marks or terrain changes (erosion, sediment), while pre-existing LiDAR DEMs improve the georeferencing of flood maps and hazard modeling. Three-dimensional city models and building footprints combined with LiDAR enable 3D flood visualization, including immersive and augmented-reality applications that support communication with decision-makers and the public [78,79].

Nonetheless, LiDAR faces well-known constraints: occlusions from buildings or vegetation, limited temporal coverage, and potential vertical errors. These issues are particularly

critical in dense urban areas, where elevation accuracy strongly affects flood predictions [75]. Despite such challenges, LiDAR remains a valuable reference in operational platforms such as Copernicus EMS, where available datasets are used to refine SAR- and optical-based flood extents, especially along complex shorelines and drainage systems [80]. Integration strategies include the following: (i) merging LiDAR with optical/SAR imagery to derive hydrologically corrected DEMs; (ii) resampling high-resolution LiDAR to match EO sensor resolution; and (iii) exploiting terrain indices (e.g., HAND, slope, curvature) in hybrid EO–ML models for flood detection and depth estimation. Where LiDAR is not openly available, alternatives such as ICESat-2 photon data or photogrammetric DSMs provide partial substitutes, though usually at lower accuracy. The fusion of LiDAR with multi-source EO data thus combines spatial detail with the temporal responsiveness required for emergency mapping.

Ancillary datasets, including land use/land cover products (e.g., CORINE, ESA WorldCover), building footprints (e.g., OpenStreetMap), infrastructure networks, and river systems, provide essential context to refine flood classification and impact analysis [81–84]. They are particularly useful in urban areas, where they help distinguish water from low-reflectance surfaces such as asphalt or burn scars [85]. Hydrological and meteorological inputs, such as GPM rainfall, runoff models, and historical flood archives, further support multi-hazard preparedness and early response [86].

Multi-source integration has therefore become standard practice. Operational services combine SAR and optical imagery with DEMs and land cover datasets to produce timely, accurate flood maps [86]. During the 2022 Pakistan floods, for instance, the fusion of Sentinel-1 SAR, Sentinel-2 land cover, and GPM precipitation data captured over 2.5 million hectares of inundation and crop losses [87]. Similarly, Copernicus EMS routinely merges SAR and optical data to refine delineation and validate rapid mapping outputs [88].

In summary, no single EO dataset can address all flood conditions. The fusion of optical, radar, thermal, topographic, and contextual information provides a robust foundation for emergency mapping. As sensor availability and data accessibility improve, integrated approaches will remain central to advancing both rapid response and long-term risk reduction.

3.2. Processing Pipelines and Methodological Approaches

Effective flood emergency mapping requires not only good data but also robust processing workflows to convert raw observations into accurate flood extent information. Over the years, a suite of processing methods has evolved, from simple image thresholding techniques to advanced AI-driven classification and data assimilation models.

Pre-processing and image enhancement: Pre-processing ensures EO data are analysis-ready, including radiometric/atmospheric corrections, orthorectification, cloud/shadow masking for optical, and calibration, speckle filtering, and terrain correction for SAR. Platforms such as Copernicus GFM or Google Earth Engine now automate these steps at scale.

Threshold-based flood detection: *Thresholding* remains a baseline due to simplicity and speed [71]. Optical approaches apply NDWI/MNDWI thresholds, while SAR flood detection often relies on change detection in pre/post-event backscatter. Adaptive methods (e.g., Otsu, Gaussian mixtures) improve performance in heterogeneous scenes. Copernicus EMS still uses semi-automated thresholding refined by post-processing, while early SAR algorithms (e.g., Long et al., 2014) exemplify this approach [71,89].

Classification and machine learning approaches: Supervised classifiers (e.g., tree-based or kernel-based methods) leverage multi-spectral, temporal, and contextual features to improve detection [90]. Copernicus EMS applied a Random Forest on Sentinel-1 during the

2023 Emilia-Romagna flood to refine extents, showing how ancillary data (elevation, land use) enhance accuracy.

Deep learning and AI-based segmentation: Deep learning has become a game-changer for flood mapping. CNN-based models (e.g., U-Net variants) capture spatial context better than pixel-wise methods, with global systems like WorldFloods detecting water even under thin clouds [91–94]. Attention-based CNNs on Sentinel-1 show improved performance in vegetated areas [95,96]. Yet, generalizability and uncertainty remain challenges, addressed by probabilistic and physics-informed approaches [97,98].

Validation and error handling: Validation is critical in emergency contexts, where errors have direct consequences [99]. Automated flood maps are prone to omission and commission errors, particularly in urban or vegetated areas, so ground truth, aerial surveys, or historical maps are used whenever possible [100]. Open reference datasets (e.g., UNOSAT, GRSS competitions) now enable objective benchmarking [101]. In practice, hybrid workflows are common: Copernicus EMS refines semi-automated outputs through expert review [57], while global systems like GFM rely on extensive pre-deployment validation [102]. Reported CSI scores of 70–80% demonstrate robust performance but also reveal typical errors, such as over-detection in radar shadows or under-detection in narrow channels [103,104].

In summary, operational flood mapping workflows strike a balance between automation and expert validation: thresholding ensures speed, machine learning enhances robustness, and deep learning pushes accuracy, while validation and hybrid approaches remain essential for reliability in crisis response.

4. Innovative Methods for 3D Flood Mapping and AI-Based Automation

4.1. Topographic and Elevation-Based Methods for Floodwater Depth Estimation

A key class of rapid flood-mapping approaches combines satellite-derived flood extents with Digital Elevation Models (DEMs) to estimate water depth, providing a computationally efficient alternative to full hydrodynamic simulations. These GIS-based methods reconstruct a water surface from the inundation outline and subtract terrain elevation to derive depth. They are fast, rely on readily available inputs (flood map + DEM), and thus are well suited for emergency response [105–107].

One of the earliest and most widely used tools is the Floodwater Depth Estimation Tool (FwDET) [105]. It interpolates a water surface from flood boundaries and subtracts the DEM to estimate depth, with Mean Absolute Errors (MAE) typically around 0.2–0.3 m. FwDET v2.0 introduced an "open-boundary" scheme for coastal floods [106], and a Google Earth Engine (GEE) implementation now enables continental-scale analyses [107]. Despite widespread uptake (e.g., in NASA's ARIA system), the method remains sensitive to DEM quality and misalignments, often leading to under- or overestimation [108].

To mitigate noise, the tool includes optional post-processing features like slope-thresholding and smoothing [77]. A critical limitation remains: the method's accuracy is highly dependent on the quality of the input DEM and the precision of flood boundary delineation, as errors in shoreline extraction propagate directly into water depth estimates [107].

To improve realism, newer approaches integrate hydrologic logic and topographic indices. RICorDE [109] incorporates the Height Above Nearest Drainage (HAND) index to prune implausible flood extents and interpolate a spatially variable water surface. Tests in Canada showed improved performance in riverine contexts compared to FwDET. Similarly, FLEXTH [77] applies morphological propagation to extend flood extents into no-data zones (e.g., clouds, radar shadow), producing smooth water surfaces that closely match hydrodynamic models. FLEXTH has shown superior accuracy and efficiency over FwDET-

GEE and is being evaluated for integration in Copernicus workflows [77]. More recently, INFLOS [110], now operational within CEMS Rapid Mapping, refines boundary samples through iterative filtering and interpolation, producing high-resolution, robust depth products validated across diverse flood scenarios [110].

A further development is EXFLOS [111], under testing by SERTIT for Copernicus EMS. It extends DEM-based depth estimation by combining flood polygons with ancillary data (e.g., hydrometric markers, field reports) to better handle occlusions and complex terrains. Still experimental, it illustrates the trend towards hybrid algorithms that balance speed with physical plausibility [111].

Despite these advances, all DEM-based tools remain constrained by topographic accuracy as highlighted also in Table 2. Even small vertical errors in DEMs (decimeters) can propagate into significant depth biases, especially in flat or urban landscapes where subtle elevation differences control inundation [107]. High-resolution LiDAR mitigates this but is rarely available at the temporal and spatial coverage required for emergencies. Likewise, EO-derived flood extents are incomplete under clouds, vegetation, or urban occlusions [77]. The most promising direction is therefore multi-source integration, where DEM-based interpolation is calibrated with complementary data (gauges, field surveys, crowdsourcing). Embedding such hybrid validation in operational workflows (e.g., INFLOS cross-checked with gauge data in CEMS) will allow rapid depth products to combine automation with the reliability needed for emergency decision-making [110,111].

Overall, DEM-based depth estimation tools such as FwDET, INFLOS, and FLEXTH have significantly advanced rapid flood mapping, but their performance remains strongly constrained by DEM accuracy and input quality. This motivates the integration of more automated, data-rich approaches—discussed in the following section—that combine geomatic methods with AI and multi-source information to improve reliability in complex environments.

Table 2. Comparison of recent DEM-based floodwater depth estimation tools used in satellite flood mapping workflows. N/A refers to data not available.

Tool	Version	Algorithm	Applicability	Computational Efficiency	RMSE	Output Characteristics	Strengths (Operative Context)	Weaknesses (Operative Context)	Main References
INFLOS	2023	Natural Neighbor interpolation with boundary filtering and iterative densification	Riverine, urban, and mixed flood scenarios (validated on 14 case studies)	<5 min for a ~100 km2 AOI; up to ~30 min for large complex AOIs	~0.1–0.3 m	Smooth interpolated water surface; raster and vector depth products	Fast, robust, no need for parameter tuning; directly integrated in Copernicus (CEMS-RM); suitable for operational use	Sensitive to DEM quality; performance may decline in highly fragmented or noisy AOIs	[110]
FwDET	v1.0 (2018)	Nearest neighbor elevation interpolation via iterative nearest-boundary assignment	Riverine floods; coastal flooding (limited applicability)	Low efficiency due to iterative calculations; slow for large AOIs	N/A	Basic raster water depth map; assumes flat water surface	Simple to implement; widely adopted in early flood mapping studies	Inaccurate for coastal/open boundary floods; ignores internal water bodies; can both over- and under-estimate, depending on DEM/polygon misalignments	[105]
FwDET	v2.0 (2019)	Cost-allocation routine replaces the nearest neighbor with a flood-edge cost-distance interpolation	Riverine and coastal flooding	Up to 15× faster than v1.0; linear (non-iterative) computational time	N/A	Raster water depth map; improved boundary handling	Supports open-boundary (coastal) floods and internal water bodies; better scalability	Integer-only DEM inputs needed; artifacts in complex terrain; retains strong DEM dependency	[106]
FwDET-GEE	v2 (2022)	Google Earth Engine implementation of FwDET v2.0	Large-scale mapping (regional to continental); multi-event analysis	~9 min for moderate AOIs (e.g., Brazos flood); up to ~7.6 h for large, high-resolution AOIs	N/A	Raster depth products in cloud-native format; optimized for GEE environment	Highly scalable for batch processing; suitable for systematic monitoring; leverages cloud resources	Long runtimes for very high-res inputs; inherits FwDET assumptions; minor artifacts under complex hydrology	[107]

Table 2. *Cont.*

Tool	Version	Algorithm	Applicability	Computational Efficiency	RMSE	Output Characteristics	Strengths (Operative Context)	Weaknesses (Operative Context)	Main References
FLEXTH	2024	Morphological edge propagation with topographic constraints (OpenCV-based)	Riverine floods (Spain, Texas test cases); suitable for cloud-obscured events	~30 s for small AOIs (e.g., Brazos flood); ~45 min for large domains; faster than FwDET GEE	~0.18 m	Water depth and water level raster maps; explicit interpolation into unmapped gaps	High accuracy for water level reconstruction; fills missing flood areas; fully open-source; real-time capable for large areas	Very sensitive to DEM vertical accuracy; integration into CEMS RM under evaluation; dependent on accurate perimeter extraction	[77]
EXFLOS	Prototype (2024)	Multi-step surface interpolation from flood polygons with optional use of hydrometric markers and social media inputs	Experimental use in CEMS Rapid Mapping; tested in urban and mixed settings (EMSR492, EMSR708, EMSR692, EMSR756)	Variable; not yet benchmarked, designed for rapid application	N/A	Raster flood depth maps; optionally vectorized; smoothed water surface	Flexible framework; can ingest heterogeneous sources (e.g., social media, field reports); intuitive interpolation process	Still under development; lacks peer-reviewed validation; performance variability not yet fully assessed	[111]

4.2. Machine Learning for Flood Susceptibility and Water Depth Estimation

Machine learning (ML) techniques—particularly "shallow" algorithms such as Random Forests (RF), Support Vector Regression (SVR), Gradient Boosting Regressors (e.g., XGBoost), and Multi-Layer Perceptrons (MLPs)—have been increasingly applied to flood mapping problems as data-driven surrogates or complements to physical models [112]. These approaches rely on training data (historical floods or simulations) to learn statistical relationships between environmental and hydrological predictors and flood occurrence or depth [113–115].

One of the first uses of ML in this domain was flood susceptibility mapping, which estimates the long-term probability of inundation based on static predictors such as elevation, slope, rainfall, soil type, and historical flood records. Such maps are pre-disaster products, useful to identify flood-prone zones, prioritize field validation, or guide satellite tasking in data-scarce regions. However, susceptibility approaches are static and region-specific, reflecting past rather than current hydrological conditions, and their accuracy strongly depends on the representativeness of training data. Consequently, they are better suited as complementary layers in decision-making rather than substitutes for event-driven mapping.

A more recent and operationally relevant development is the use of ML regression models for event-specific flood depth estimation. In this framework, ML is trained on libraries of simulated or observed floods, learning how forcing conditions such as rainfall, discharge, and terrain features translate into inundation extent and depth. For instance, MaxFloodCast [116] was trained on thousands of synthetic scenarios for Harris County (Houston), producing near-real-time predictions of peak flood depth with $R^2 \approx 0.95$ and RMSE ≈ 0.19 m. During Hurricane Harvey, its forecasts closely matched observed flood maps, showing how physics-informed ML surrogates can rival hydrodynamic simulations at a fraction of the computational cost. Similar approaches with RF, SVR, or MLP regressors have achieved rapid predictions in seconds instead of hours [117,118]. These "train-offline, predict-online" strategies are extremely promising for emergency response, though they require extensive training datasets and remain largely site-specific. Transferability to new regions or unprecedented hydrological conditions is still an open challenge.

Liou and Hoang (2024) [112] addressed this by combining FwDET outputs with regression models trained on 804 in situ depth observations from the 2020 Nhat Le flood. Their Random Forest improved R^2 from 0.721 to 0.933 and reduced RMSE from 0.729 m to 0.181 m, demonstrating how hybrid methods can dramatically refine geometric depth

estimations. Yet, even residual errors around 0.2 m may remain critical in shallow-flood scenarios, underscoring the need for continuous validation.

In operational rapid mapping, tools like INFLOS and FLEXTH are still indispensable due to their computational efficiency, but their outputs may suffer in complex topography or fragmented floodplains. A promising direction is the integration of lightweight ML correction layers on top of such geometric methods, balancing speed and accuracy. Moving forward, challenges include automating feature extraction, developing retraining strategies to keep models updated, and incorporating uncertainty quantification to make ML-based flood depth estimates reliable in real-world crisis response.

Beyond these case studies, a wide range of algorithms—from SVM classifiers [119], to RF [120], to hybrid approaches like ANFIS [121] and ensemble decision trees [122]—have been explored for flood delineation, susceptibility, and depth estimation. These diverse applications illustrate both the adaptability of ML across contexts and the need for careful tailoring to regional data availability and operational requirements.

Elkhrachy (2022) [123] investigated multiple regression models (GBR, RFR, KNR, SVR, MLP) for flash-flood depth estimation in Egypt, using Sentinel-1 SAR, Sentinel-2 optical, DSM, and land-use layers. Trained on over 250,000 synthetic HEC-RAS outputs, the models achieved RMSE $\approx$ 0.18–0.22 m for shallow floods (<1 m). While these results confirm ML's capacity to approximate water depths, they also highlight limitations: errors of a few decimeters can substantially alter mapped inundation extent in flat terrain, and biases in synthetic training data propagate directly into the predictions.

Table 3 summarizes key studies, their algorithms, datasets, and findings.

Table 3. Summary of machine learning approaches for flood delineation, susceptibility, and water depth estimation.

Algorithm	Study (Year)	Country	EO Data Source and Auxiliary Inputs	Main Findings
Support Vector Machine (SVM)	Tanim et al. (2022), [119]	Indonesia	Sentinel-1 GRD (VV, VH polarization), local high-resolution DEM.	SVM reliably separated flooded vs. non-flooded urban pixels, showing higher accuracy than RF.
Random Forest (RF)	Composto et al. (2024), [120]	USA (Louisiana)	Sentinel-2 MSI (10 m bands), 30 m DEM, 10 m land-cover map, NDWI, NDVI.	RF accurately mapped Hurricane Ida inundation, with improved performance in urban areas using DEM derivatives.
Adaptive Neuro-Fuzzy Inference System (ANFIS)	Razavi Termeh et al. (2018), [121]	Iran	GIS/RS layers (30 m DEM derivatives: slope, curvature, TWI; land use; soil type; rainfall frequency).	ANFIS produced regional susceptibility maps consistent with historical records, highlighting slope and TWI as key predictors.
Deep Boost (ensemble of decision trees)	Chakrabortty et al. (2021), [122]	Bangladesh	Multi-temporal optical indices (NDVI, NDWI), SRTM DEM (30 m), soil moisture proxies.	Deep Boost slightly outperformed MLP, with diminishing gains beyond certain tree depth
Gradient Boosting Regression (GBR)	Elkhrachy (2022), [123]	Egypt	Sentinel-1 SAR backscatter (VV, VH), Sentinel-2 MSI bands, Copernicus DSM (30 m)	GBR predicted flood depths with high accuracy; SAR backscatter and DSM elevation were the most important features.
Random Forest Regression (RFR)	Liou & Hoang (2024), [112]	Vietnam	Sentinel-1 GRD (VV, VH), 5 m LiDAR DEM (resampled 10 m), terrain indices (slope, TWI, SPI), 24 h rainfall, 10 m land cover.	RFR improved depth estimation over FwDET, proving operationally efficient on cloud infrastructure
Support Vector Regression (SVR)	Elkhrachy (2022), [123]	Egypt	Sentinel-1 SAR (VV, VH), Sentinel-2 MSI (NDWI, NDSI), Copernicus DSM (30 m), land cover.	SVR achieved depth accuracy comparable to GBR, effective for non-linear relationships with limited training data
K-Nearest Neighbors Regression (KNR)	Elkhrachy (2022), [123]	Egypt	Sentinel-1 SAR (VV), Sentinel-2 MSI (NDWI), Copernicus DSM (30 m), land cover.	KNR predicted flood depths with good accuracy but was computationally slower in complex terrain.
Multi-layer Perceptron Regression (MLPR)	Elkhrachy (2022), [123]	Egypt	Sentinel-1 SAR (VV, VH), Sentinel-2 optical (B3, B4, B8), Copernicus DSM (30 m), land cover.	MLPR captured non-linear EO–depth relationships, achieving high accuracy with careful parameter tuning.

4.3. Deep Learning Models for Flood Extent Detection

Deep learning (DL) has gained prominence in flood mapping over the past few years, extending machine learning (ML) by employing multi-layered neural networks that can automatically extract complex patterns from large datasets. Unlike traditional ML methods that depend on hand-crafted features, DL directly ingests raw data such as satellite images, time series, or gridded spatial information, and identifies relevant features

for flood detection and prediction. Commonly applied architectures include convolutional neural networks (CNNs), recurrent neural networks (RNNs, particularly LSTMs), and fully connected networks, often combined in hybrid models. A review by Bentivoglio et al. (2022), covering 58 publications, highlights the rapid adoption of DL for flood delineation, susceptibility mapping, and real-time forecasting, with many studies reporting improved accuracy compared to conventional methods [115]. DL models typically rely on five major categories of input data:

1. Topographical information such as DEMs and terrain derivatives including slope, curvature, and aspect;
2. Meteorological data such as rainfall intensity and duration obtained from gauges or satellites;
3. Geological and soil parameters including infiltration rates and soil types;
4. Geographical data layers derived from remote sensing such as land cover, NDVI, and proximity to water bodies;
5. Anthropogenic information such as built environment indicators, road networks, and urban density.

Sensitivity analyses consistently show that topographical predictors, especially slope, land cover, terrain curvature, and distance to watercourses, are among the most influential factors for DL-based flood models [124–127].

Convolutional Neural Networks (CNNs). CNNs are the dominant DL architecture for flood mapping tasks because of their ability to recognize spatial patterns. Convolutional filters capture local context and texture, making CNNs well suited for classifying flooded versus non-flooded areas in satellite imagery. Wieland and Martinis (2019) demonstrated the advantages of CNNs with a pipeline for Sentinel-2 multi-spectral images, which significantly outperformed both rule-based classifications and traditional ML methods such as SVMs [58,128]. CNNs are widely used in binary flood mapping but have also been adapted to regression tasks, for example predicting water depth directly from SAR backscatter intensity combined with a DEM. Early studies suggest CNN regressors can approximate water depth if sufficient training data are available. Other works employ 2D and even 3D CNNs on spatiotemporal datasets to produce flood hazard maps, learning from many simulated scenarios to estimate the probability or depth of flooding over a grid. A key limitation of CNNs is the demand for large labeled datasets. Training flood segmentation models requires hundreds or thousands of paired images and reference flood masks. Initiatives such as the IEEE GRSS flood mapping competitions and curated datasets like Sen1Floods11 have been instrumental in addressing this need. Transfer learning, where CNNs pre-trained on generic image databases are fine-tuned for flood mapping, has also proven effective in reducing the data burden and improving generalization.

Recurrent Neural Networks (RNNs) and LSTMs: RNNs are designed to model sequential dependencies and therefore play a complementary role in flood mapping. They are primarily used for hydrological forecasting and rainfall–runoff modeling, capturing temporal patterns in rainfall, river discharge, or water level time series. In flood applications, RNNs and LSTMs have been combined with spatial encoders to predict the temporal evolution of flood inundation. For instance, Kao et al. (2021) implemented an encoder–decoder architecture where an LSTM processed rainfall sequences and produced a latent representation that was decoded into flood features [59,60,129]. Graph-based RNNs have also been applied to drainage networks, predicting which streets are likely to flood under given rainfall scenarios [130]. Although RNNs alone are not typically used for static flood mapping, they are effective when temporal dynamics must be modeled. Hybrid models combining CNNs for spatial encoding and LSTMs for temporal sequencing are

emerging as promising solutions, though they remain mostly experimental in operational contexts [131,132].

Multi-Layer Perceptrons (MLPs) and Other Networks: MLPs, consisting of stacked fully connected layers, are sometimes classified as DL models when they include multiple hidden layers. In flood mapping they are usually used either as benchmark baselines or as modules within more complex architectures. Earlier susceptibility mapping studies employed MLPs to integrate rainfall, terrain, and soil factors into flood risk scores, but they generally underperform compared to CNNs for image-based classification [125]. Nonetheless, MLPs are valuable as simple encoders or decoders within hybrid models and have been used in conjunction with optimization algorithms such as genetic algorithms or particle swarm optimization for improving susceptibility or hazard mapping [133,134]. Beyond MLPs, deep generative models such as autoencoders and GANs have recently been explored to generate synthetic flood scenarios or to downscale coarse flood maps to higher resolution, showing that DL in this field is diversifying.

Comparisons and performance. Across studies, CNN-based approaches consistently outperform traditional thresholding, GIS-based methods, and shallow ML classifiers in flood extent mapping, particularly in complex environments such as urban or vegetated areas [58,127,134]. In surrogate modeling of hydraulic simulations, DL has also shown striking efficiency gains. MLP-based surrogates have achieved extremely low RMSE values (as low as 0.0013 m) with computational speed-ups exceeding 1000×, while CNN-based surrogates have reduced the mean absolute error below 1 m while achieving efficiency improvements of up to 2000×. LSTM-based surrogates, when coupled with reduced-order hydrodynamic models, have reached RMSE values around 0.01 m with speed-ups of approximately 1500× [115]. These results demonstrate the capacity of DL not only to enhance flood mapping accuracy but also to approximate computationally expensive simulations at operationally relevant speeds.

Challenges. Despite this progress, several technical barriers limit the widespread operational use of DL in flood mapping. The first is the need for extensive, diverse, and accurately labeled training datasets that capture a wide range of hydrological and geographical conditions. The scarcity of high-quality ground truth data remains a bottleneck. A second challenge is computational cost: while inference is rapid once a model is trained, the training process itself can require substantial resources. A third limitation concerns generalization. Many DL models show strong performance in the region or event where they were trained but fail to transfer effectively to new locations or unprecedented flood scenarios. Domain adaptation, transfer learning, and pre-trained generalized architectures are therefore crucial avenues of research. Finally, most DL approaches remain deterministic; probabilistic frameworks and uncertainty quantification are still underdeveloped, yet they are critical for supporting decision-making in emergency contexts. These trends are further illustrated in Table 4, which summarizes selected DL studies across different data sources and flood mapping tasks.

In summary, classical machine learning methodologies have established an essential foundation for flood mapping, yet contemporary deep learning techniques—particularly Convolutional Neural Networks (CNNs) and Recurrent Neural Networks (RNNs)—have demonstrated significant improvements in terms of predictive accuracy, computational scalability, and efficiency. Furthermore, hybrid approaches integrating deep learning predictions with traditional hydrological and physical modeling datasets are increasingly recognized for their capability to enhance operational flood risk assessments.

Despite these advancements, several critical technical challenges hinder the broader operational deployment of deep learning models. Foremost among these challenges is the requirement for extensive and representative training datasets, capturing diverse

geographic and hydrological conditions. The scarcity and high cost of obtaining comprehensive, accurately labeled flood event data significantly restrict the applicability of deep learning approaches. Moreover, the substantial computational resources needed for the initial training phase of deep learning models pose significant constraints, particularly in emergency response scenarios demanding rapid deployment. Consequently, pre-trained or generalized model architectures are essential for immediate applicability. Another major technical limitation involves the issue of model generalization and transferability; models calibrated on specific flood scenarios or localized events typically exhibit limited predictive performance when applied to geographically distinct or novel flooding situations. Addressing this limitation necessitates rigorous research focused on enhancing model generalization capabilities through more diverse, comprehensive, and systematically structured training datasets.

Table 4. Summary of AI-based models for flood mapping, datasets used, and reported performance metrics.

Algorithm and Data	Key Studies and Results
CNNs—Satellite Imagery	Nogueira et al. (2018) [131]; Kang et al. (2018) [132]; Sarker et al. (2019) [133]; Nemni et al. (2020) [134]; Isikdogan et al. (2017) [135]; Wieland & Martinis (2019) [128]; Zhao et al. (2021c) [136]. Studies showed CNNs effectively mapped floods across diverse sensors (Landsat, Sentinel, urban RS), generally outperforming traditional classifiers
CNNs—UAV Imagery (High-Res Local Mapping)	Gebrehiwot et al. (2019) [137]; Ichim & Popescu (2020) [138]; Hashemi-Beni et al. (2021) [139]. UAV-based CNNs achieved high accuracy in detailed local flood mapping, supporting rapid assessment in urban/rural test sites.
CNNs—Laboratory/Model-Based Applications	Hou et al. (2021) [140]; Guo et al. (2021) [141]; Kabir et al. (2020) [142] CNNs were integrated with physical/lab models (e.g., LISFLOOD-FP, CAD-DIES), showing strong potential for simulating flood propagation and hazard mapping.
CNNs—Integrated with Other Algorithms/Factors	Lei et al. (2021) [143]; Fang et al. (2020a) [125]; Khosravi et al. (2020) [124]; Panahi et al. (2021) [91]. Hybrid CNN approaches (CNN + RNN, CNN + LSTM, conditioning factors) improved flood detection and susceptibility mapping in diverse regions (South Korea, China, Iran).
Multi-Layer Perceptrons (MLPs)	Li et al. (2015) [144]; Li et al. (2016a) [145]; Chu et al. (2020) [146]. MLPs, sometimes optimized with genetic/particle swarm algorithms, were applied with Landsat and hydraulic models for flood susceptibility and depth estimation.

5. Discussion

This review examined the state of EO-based flood depth estimation, comparing physical GIS-based approaches with data-driven ML/DL techniques. The objective was not only to summarize methods but also to critically assess their operational value, trade-offs, and future potential for rapid flood mapping.

Best practices. A consistent finding across studies is that combining multiple EO data sources improves robustness. SAR provides all-weather flood delineation, while optical imagery can add detail in cloud-free conditions, and high-quality DEMs remain indispensable for depth estimation [84,105,115]. ML and hybrid models benefit from topographic derivatives (e.g., slope, TWI), which reduce false positives particularly at urban–rural transitions [112,120]. Open-access datasets (e.g., Sentinel, Copernicus DEM) and open-source algorithms deployed on cloud or HPC infrastructures enable scalable and reproducible workflows [84,105]. However, even these "best practices" highlight contrasting strengths: GIS-based methods offer interpretability and immediate applicability with minimal training data, while ML/DL approaches demonstrate higher accuracy and adaptability once sufficient training samples exist [147,148]. Importantly, expert validation remains essential to correct artifacts and refine outputs in operational settings [105]. Communication of uncertainty—through quality flags or confidence layers—should be considered a best practice, but is rarely implemented in practice [80,115].

Technical gaps. Despite clear progress, several technical limitations continue to constrain the accuracy and operational value of EO-based flood depth estimation. A first challenge concerns the quality and consistency of input data. DEM artifacts, outdated elevation models, and errors in flood extent masks propagate directly into depth estimates, leading to systematic biases [105]. Physical GIS-based methods are particularly sensitive to DEM vertical accuracy and resolution, while data-driven approaches often inherit noise and

false positives from the training labels [115]. Urban areas remain especially problematic: without high-resolution LiDAR or detailed DSMs capturing buildings and drainage networks, both physical and ML/DL models systematically underestimate flood depth [115]. A second gap lies in generalization across regions and events. While DEM-based methods provide consistent but coarse results anywhere a DEM is available, most ML/DL models are trained for specific catchments or flood types and perform poorly when transferred to new hydrological settings [115]. This reflects a broader trade-off: physics-driven methods are less accurate but inherently more generalizable, whereas ML/DL models can achieve higher precision but often fail outside their calibration domain. A third issue is the absence of systematic uncertainty quantification. Physical methods rarely propagate DEM or remote-sensing errors into confidence intervals, while most ML/DL frameworks provide deterministic outputs without probability estimates [115]. This lack of uncertainty communication reduces trust and hampers integration into decision-making workflows. In addition, computational cost and data requirements remain significant barriers for deep learning. Training CNNs or hybrid DL architectures often requires extensive GPU resources and large volumes of labeled flood maps, which are costly and difficult to acquire [115]. Public initiatives such as Sen1Floods11 and benchmarking efforts are helping, but training data remain sparse and geographically biased, limiting model robustness and transferability. Finally, hydrological consistency is not always enforced. Purely EO-based or ML-generated maps may capture flood extents that visually match satellite data but violate physical constraints, such as flow direction or volume continuity [105,115]. This issue limits their acceptance in operational hydrology and highlights the need for hybrid models that embed physical rules into data-driven frameworks

Current operational approaches. For near-real-time applications, DEM-based methods such as INFLOS and FLEXTH currently provide the most reliable balance of robustness and scalability [105], particularly when complemented by lightweight ML refinement trained on representative local or simulated data [112,123]. The implementation of open, cloud-based workflows could support wider accessibility, reproducibility, and rapid deployment in diverse regions [84,105]. Including basic uncertainty indicators (e.g., cloud cover masks, DEM quality scores) would enhance the interpretability and reliability of flood depth products [115].

When compared with earlier reviews, a clear distinction emerges. Traditional reviews and methodological studies on flood modeling and risk assessment [149–151] primarily emphasized large-scale hydraulic and hydrodynamic simulations, highlighting their accuracy but also their high computational cost and limited real-time applicability. More recent reviews focusing on machine learning and hazard mapping [151,152] underlined the promise of data-driven methods, but often with a stronger emphasis on susceptibility or hazard layers rather than operational flood depth products. In contrast, our synthesis highlights that EO-based depth estimation is beginning to bridge these domains, combining the robustness of DEM-based physical approaches with the scalability of ML/DL surrogates.

This positioning underscores the novelty of EO-based operational approaches: they are not intended to replace hydrodynamic models or hazard mapping frameworks but rather to complement them by providing rapid, spatially explicit depth estimates during emergencies. The current operational frontier is therefore defined by pragmatic workflows—cloud-based, open-access, hybrid, and uncertainty-aware—that allow EO flood depth mapping to move from research to deployment.

Future perspectives. Research priorities for EO-based flood depth estimation converge toward hybrid methodologies that embed physical constraints into ML architectures or employ ML surrogates for physics-based models, thereby combining computational efficiency with physical realism [112,116]. The emergence of generalized “foundation models,”

trained on large and diverse flood datasets (e.g., FloodCastBench), holds promise for reducing the need for region-specific retraining [146]. Advances in high-resolution EO sensors and 3D urban datasets are expected to significantly improve the accuracy of fine-scale mapping, addressing a persistent gap for urban flood assessment [115]. Near-real-time assimilation of heterogeneous data streams—including EO imagery, ground sensors, hydrological forecasts, and even crowdsourced observations—could shift flood mapping from a reactive process to a proactive capability that anticipates evolving inundation dynamics [80,84,148].

A critical comparative insight is that while previous reviews [149–151] have emphasized flood hazard modeling and susceptibility assessment, they rarely addressed the specific challenge of flood depth estimation from EO. Our analysis highlights that despite the rapid rise of DL-based approaches, issues of model transferability and uncertainty quantification remain unresolved. Explicit operationalization of uncertainty—through ensemble modeling, Bayesian inference, or probabilistic DL outputs—would allow the development of products that better support risk-based decision-making [115,148]. Addressing these limitations requires coordinated efforts toward standardized benchmarking datasets, shared open-source tools, and collaborative validation campaigns across multiple geographies.

6. Conclusions

EO-based flood depth estimation has rapidly evolved from basic GIS interpolation methods to advanced hybrid and deep learning approaches. While earlier reviews and articles tended to focus either on hydrodynamic modeling [149,150] or on machine learning for flood susceptibility and hazard assessment [151,152], our synthesis highlights the operational middle ground now emerging: scalable EO-based workflows capable of producing near-real-time flood depth estimates.

This distinct perspective underscores the value of EO approaches not as replacements for hydraulic simulations or hazard mapping, but as complementary tools that bring speed, scalability, and global coverage to crisis contexts. At the same time, challenges remain substantial: the generalization of ML/DL models across diverse geographies, the integration with forecasting systems, and the systematic treatment of uncertainty all require further research [115,147,148].

Ultimately, the path forward lies in strengthening hybrid methods that combine the physical realism of models with the efficiency of ML surrogates, advancing generalizable architectures such as foundation models, and embedding uncertainty quantification as a standard output. By critically situating EO-based flood depth mapping within the broader modeling landscape, this review emphasizes its growing role in supporting operational decision-making during flood emergencies.

Author Contributions: T.D.: Conceptualization, Methodology, Validation, Formal Analysis, Investigation, Data Curation, Visualization, Writing—Original Draft, Writing—Review and Editing. S.G.: Conceptualization, Methodology, Validation, Formal Analysis, Investigation, Data Curation, Writing—Original Draft, Writing—Review and Editing. P.B.: Conceptualization, Validation, Resources, Supervision, Project Administration, Writing—Review and Editing. V.F.: Validation, Resources, Supervision, Project Administration, Writing—Review and Editing. All authors have read and agreed to the published version of the manuscript.

Funding: This study was carried out within the Space It Up project funded by the Italian Space Agency, ASI, and the Ministry of University and Research, MUR, under contract n. 2024-5-E.0-CUP n. I53D24000060005.

Acknowledgments: The authors would like to thank the SDG11lab at Politecnico di Torino and ITHACA S.r.l. for their support and collaboration during the preparation of this work. Special thanks are extended to the Copernicus Emergency Management Service (CEMS) community for making operational data and documentation publicly available, which was valuable for this review.

Conflicts of Interest: Author Tommaso Destefanis has received a PhD scholarship from Company Ithaca s.r.l.. Author Vanina Fissore was employed by the company Ithaca s.r.l.. The remaining authors declare that the research was conducted in the absence of any commercial or financial relationships that could be construed as a potential conflict of interest.

References

1. Liu, Q.; Du, M.; Wang, Y.; Deng, J.; Yan, W.; Qin, C.; Liu, M.; Liu, J. Global, Regional and National Trends and Impacts of Natural Floods, 1990–2022. *Bull. World Health Organ.* **2024**, *102*, 410–420. [CrossRef]
2. Ritchie, H.; Rosado, P.; Roser, M. Natural Disasters. Our World in Data. 2022. Available online: https://ourworldindata.org/natural-disasters (accessed on 3 July 2025).
3. Tavus, B.; Kocaman, S.; Gokceoglu, C.; Nefeslioglu, H.A. Considerations on the Use of Sentinel-1 Data in Flood Mapping in Urban Areas: Ankara (Turkey) 2018 Floods. *Int. Arch. Photogramm. Remote Sens. Spat. Inf. Sci.* **2018**, *XLII-5*, 575–581. [CrossRef]
4. Dasgupta, A.; Grimaldi, S.; Ramsankaran, R.A.; Pauwels, V.R.; Walker, J.P.; Chini, M.; Hostache, R.; Matgen, P. Flood mapping using synthetic aperture radar sensors from local to global scales. In *Global Flood Hazard: Applications in Modeling, Mapping, and Forecasting*; Schumann, G.J.-P., Bates, P.D., Apel, H., Aronica, G.T., Eds.; Geophysical Monograph Series; John Wiley & Sons, Inc.: Hoboken, NJ, USA, 2018; pp. 55–77. [CrossRef]
5. Iselborn, K.; Stricker, M.; Miyamoto, T.; Nuske, M.; Dengel, A. On the importance of feature representation for flood mapping using classical machine learning approaches. *arXiv* **2023**, arXiv:2303.00691. [CrossRef]
6. Munawar, H.S.; Hammad, A.W.A.; Waller, S.T. Remote Sensing Methods for Flood Prediction: A Review. *Sensors* **2022**, *22*, 960. [CrossRef]
7. Foroughnia, F.; Alfieri, S.M.; Menenti, M.; Lindenbergh, R. Evaluation of SAR and Optical Data for Flood Delineation Using Supervised and Unsupervised Classification. *Remote Sens.* **2022**, *14*, 3718. [CrossRef]
8. European Commission Copernicus Emergency Management Service (CEMS). Copernicus EMS. Available online: http://emergency.copernicus.eu/ (accessed on 9 July 2025).
9. World Bank. Global Flood Monitoring System (GFMS)—Waterdata. Available online: https://wbwaterdata.org/dataset/global-flood-monitoring-system-gfms (accessed on 9 July 2025).
10. GIS4Schools Project. Copernicus EMS and Crisis Maps Production—Documentation. Available online: https://gis4schools.readthedocs.io/en/latest/part4/4_1.html (accessed on 3 July 2025).
11. Wania, A.; Joubert-Boitat, I.; Dottori, F.; Kalas, M.; Salamon, P. Increasing timeliness of satellite-based flood mapping using early warning systems in the Copernicus Emergency Management Service. *Remote Sens.* **2021**, *13*, 2114. [CrossRef]
12. Satriano, V.; Ciancia, E.; Pergola, N.; Tramutoli, V. A first extension of the robust satellite technique RST-FLOOD to Sentinel-2 data for the mapping of flooded areas: The case of the Emilia Romagna (Italy) 2023 event. *Remote Sens.* **2024**, *16*, 3450. [CrossRef]
13. Roth, F.; Bauer-Marschallinger, B.; Tupas, M.E.; Reimer, C.; Salamon, P.; Wagner, W. Sentinel-1-based analysis of the severe flood over Pakistan 2022. *Nat. Hazards Earth Syst. Sci.* **2023**, *23*, 3305–3317. [CrossRef]
14. Copernicus Emergency Management Service. Global Flood Awareness System (GloFAS). Available online: https://global-flood.emergency.copernicus.eu/technical-information/glofas-gfm/ (accessed on 3 July 2025).
15. Schumann, G.J.-P.; Brakenridge, G.R.; Kettner, A.J.; Kashif, R.; Niebuhr, E. Assisting flood disaster response with Earth observation data and products: A critical assessment. *Remote Sens.* **2018**, *10*, 1230. [CrossRef]
16. NASA IMERG: Integrated Multi-satellitE Retrievals for GPM. Global Precipitation Measurement Mission. Available online: https://gpm.nasa.gov/data/imerg (accessed on 11 July 2025).
17. Wu, R.A.H. *GPM Ground Validation GLOBAL flood Monitoring System (GFMS) Flood Maps IFloodS*; NASA Global Hydrometeorology Resource Center Distributed Active Archive Center: Huntsville, AL, USA, 2025. [CrossRef]
18. Adler, R.; Gu, G.; Zhou, N.; Wu, H.; Matgen, P.; Galantowicz, J.; Schumann, G.; Yilmaz, K.K. The role of satellite information in forecasting, modeling, and mapping the 2019 Mozambique flood. *J. Flood Risk Manag.* **2025**, *18*, e12843. [CrossRef]
19. Zhang, J.; Liu, K.; Wang, M. Flood Detection using Gravity Recovery and Climate Experiment (GRACE) Terrestrial Water Storage and Extreme Precipitation Data. *Earth Syst. Sci. Data* **2023**, *15*, 521–540. [CrossRef]
20. NASA LANCE—Land, Atmosphere Near real-time Capability for EOS. Earthdata. Available online: https://www.earthdata.nasa.gov/data/projects/lance (accessed on 11 July 2025).
21. UNOSAT. Preliminary Satellite-Derived Flood Assessment, Islamic Republic of Pakistan. Available online: https://unosat.org/products/3352 (accessed on 11 July 2025).

22. The Flood Observatory. Available online: https://floodobservatory.colorado.edu/ (accessed on 11 July 2025).
23. GEO/LEO/SAR Flood Pilot. CEOS | Committee on Earth Observation Satellites. Available online: https://ceos.org/ourwork/workinggroups/disasters/wgdisasters-activities/floods/ (accessed on 3 July 2025).
24. Chalifoux, R. Flood Pilot Final Report. CEOS. Available online: https://ceos.org/document_management/Meetings/SIT/SIT-32/Documents/32_Chalifoux_Flood%20Pilot%20Final%20Report_v1_20170327.pdf (accessed on 10 July 2025).
25. 2017 Flood Sri Lanka 4474. Flood Observatory. Available online: https://floodobservatory.colorado.edu/Events/2017SriLanka4474/2017SriLanka.html (accessed on 11 July 2025).
26. Global Facility for Disaster Reduction and Recovery (GFDRR). *Use of EO Satellites in Support of Recovery from Major Disasters: Taking Stock and Moving Forward*; CEOS, World Bank Group: Washington, DC, USA, 2019; Available online: https://www.gfdrr.org/sites/default/files/publication/Use_of_EO_Satellites_012322020_D_LOW-RES.pdf (accessed on 11 July 2025).
27. JAXA Earth-Graphy/Space Technology Directorate I. Sentinel Asia. Available online: https://earth.jaxa.jp/en/application/disaster/sentinel-asia/index.html (accessed on 11 July 2025).
28. Sentinel Asia. Flood, Storm in India on 17 May 2021. Available online: https://sentinel-asia.org/EO/2021/article20210517IN.html (accessed on 11 July 2025).
29. Sentinel Asia. Sentinel Asia Annual Report 2021. Available online: https://sentinel-asia.org/reports/Reports/SA_Annual_Report_2021.pdf (accessed on 7 July 2025).
30. Google. How We Are Using AI for Reliable Flood Forecasting at a Global Scale. Google Blog. Available online: https://blog.google/technology/ai/google-ai-global-flood-forecasting/ (accessed on 11 July 2025).
31. Google. How We're Helping Partners with Improved and Expanded AI-Based Flood Forecasting. Google Blog. Available online: https://blog.google/technology/ai/expanding-flood-forecasting-coverage-helping-partners/ (accessed on 11 July 2025).
32. Google Research. An Improved Flood Forecasting AI Model, Trained and Evaluated Globally. Google AI Blog. Available online: https://research.google/blog/a-flood-forecasting-ai-model-trained-and-evaluated-globally/ (accessed on 11 July 2025).
33. Microsoft. Microsoft/ai4g-Flood. GitHub. Available online: https://github.com/microsoft/ai4g-flood (accessed on 11 July 2025).
34. Copernicus EMS On Demand Mapping. Available online: https://mapping.emergency.copernicus.eu (accessed on 3 July 2025).
35. Google Research. Flood Forecasting. Available online: https://sites.research.google/gr/floodforecasting/ (accessed on 11 July 2025).
36. Service Overview | Copernicus EMS On Demand Mapping. Available online: https://mapping.emergency.copernicus.eu/about/risk-and-recovery-manual/service-overview/ (accessed on 11 July 2025).
37. Stats | Copernicus EMS On Demand Mapping. Available online: https://mapping.emergency.copernicus.eu/stats/ (accessed on 11 July 2025).
38. The Copernicus Emergency Management Service: A Global, Versatile and Operational Tool for Emergency Managers and Disaster Risk Reduction Stakeholders. Copernicus. Available online: https://www.copernicus.eu/en/news/news/observer-copernicus-emergency-management-service-global-versatile-and-operational-tool (accessed on 11 July 2025).
39. Increasing Resilience through Earth Observation | FP7. CORDIS | European Commission. Available online: https://cordis.europa.eu/project/id/312461/reporting (accessed on 12 July 2025).
40. Official Journal L 102/2018. Available online: https://eur-lex.europa.eu/legal-content/EN/TXT/HTML/?uri=OJ:L:2018:102:FULL (accessed on 12 July 2025).
41. Who Can Request the Service | Copernicus EMS On Demand Mapping. Available online: https://mapping.emergency.copernicus.eu/about/who-can-request-the-service/ (accessed on 12 July 2025).
42. How to Request the Service | Copernicus EMS On Demand Mapping. Available online: https://mapping.emergency.copernicus.eu/about/how-to-request-the-service/ (accessed on 12 July 2025).
43. Ajmar. Response to Flood Events. Geophysical Monograph Series. Available online: https://agupubs.onlinelibrary.wiley.com/doi/abs/10.1002/9781119217930.ch14 (accessed on 12 July 2025).
44. Rapid Mapping for Emergency Response Portfolio | Copernicus EMS On Demand Mapping. Available online: https://mapping.emergency.copernicus.eu/about/rapid-mapping-portfolio/ (accessed on 12 July 2025).
45. Donezar-Hoyos, U.; Albizua-Huarte, L.; Amezketa-Lizarraga, E.; Barinagarrementeria-Arrese, I.; Ciriza-Labiano, R.; de Blas-Corral, T.; Larrañaga-Urien, A.; Ros-Elso, F.; Tamés-Noriega, A.; Viñuales-Lasheras, M.; et al. The Copernicus EMS Validation Service as a Vector for Improving the Emergency Mapping Based on Sentinel Data. *Rev. Teledetección* **2020**, *56*, 56. [CrossRef]
46. Ajmar, A.; Boccardo, P.; Disabato, F.; Tonolo, F.G. Rapid Mapping: Geomatics Role and Research Opportunities. *Rend. Fis. Acc. Lincei* **2015**, *26*, 63–73. [CrossRef]
47. Global Trends in Satellite-Based Emergency Mapping. Science. Available online: https://www.science.org/doi/10.1126/science.aad8728 (accessed on 12 July 2025).
48. Rapid Mapping Manual | Copernicus EMS On Demand Mapping. Available online: https://mapping.emergency.copernicus.eu/about/rapid-mapping-manual/ (accessed on 12 July 2025).

49. Daudt, R.C.; Saux, B.L.; Boulch, A.; Gousseau, Y. Urban Change Detection for Multispectral Earth Observation Using Convolutional Neural Networks. *arXiv* **2018**, arXiv:1810.08468. [CrossRef]
50. Macchiarulo, V.; Giardina, G.; Milillo, P.; Aktas, Y.D.; Whitworth, M.R. Integrating Post-Event Very High Resolution SAR Imagery and Machine Learning for Building-Level Earthquake Damage Assessment. *Bull. Earthq. Eng.* **2024**. Available online: https://link.springer.com/article/10.1007/s10518-024-01877-1 (accessed on 12 July 2025). [CrossRef]
51. Detection Methods and Damage Assessment | Copernicus EMS On Demand Mapping. Available online: https://mapping.emergency.copernicus.eu/about/rapid-mapping-manual/detection-methods-damage-assessment/ (accessed on 12 July 2025).
52. Zhang, M.; Chen, Z.; Wang, J.; Kar, B.; Pierce, M.; Tiampo, K.; Eguchi, R.; Glasscoe, M. Optical Remote Sensing for Global Flood Disaster Mapping: A Critical Review Towards Operational Readiness. *Remote Sens.* **2025**, *17*, 1886. [CrossRef]
53. Schumann, J.-P.G. Breakthroughs in Satellite Remote Sensing of Floods. *Front. Remote Sens.* **2024**, *4*, 1280654. [CrossRef]
54. European Commission. EU Civil Protection Mechanism. Available online: https://civil-protection-humanitarian-aid.ec.europa.eu/what/civil-protection/eu-civil-protection-mechanism_en (accessed on 11 July 2025).
55. Satellite Flood Mapping Service Enhances Civil Protection in France. Innovations Report. Available online: https://www.innovations-report.com/agriculture-environment/earth-sciences/report-56913/ (accessed on 12 July 2025).
56. NRT Global Flood Products | NASA Earthdata. Available online: https://www.earthdata.nasa.gov/data/instruments/viirs/near-real-time-data/nrt-global-flood-products (accessed on 12 July 2025).
57. Floods Copernicus EMS. Available online: http://emergency.copernicus.eu/use-cases/floods-early-warning-and-monitoring/ (accessed on 12 July 2025).
58. Tarpanelli, A.; Mondini, A.C.; Camici, S. Effectiveness of Sentinel-1 and Sentinel-2 for Flood Detection Assessment in Europe. *Nat. Hazards Earth Syst. Sci.* **2022**, *22*, 2473–2489. [CrossRef]
59. Geoportale MASE. FLOOD DIRECTIVE. Available online: https://gn.mase.gov.it/portale/direttive-alluvioni (accessed on 12 July 2025).
60. Mostert, E.; Junier, S.J. The European Flood Risk Directive: Challenges for Research. *Hydrol. Earth Syst. Sci. Discuss.* **2009**, *6*, 4961–4988. [CrossRef]
61. World Bank Blogs. Flood Hazard and Risk Maps: A Key Instrument for Flood Risk Management. Available online: https://blogs.worldbank.org/en/water/flood-hazard-and-risk-maps-key-instrument-flood-risk-management (accessed on 12 July 2025).
62. Vavassori, A.; Carrion, D.; Zaragozi, B.; Migliaccio, F. VGI and Satellite Imagery Integration for Crisis Mapping of Flood Events. *ISPRS Int. J. Geo-Inf.* **2022**, *11*, 611. [CrossRef]
63. Flood Affected Area Atlas of India. Coordinates. Available online: https://mycoordinates.org/flood-affected-area-atlas-of-india/ (accessed on 12 July 2025).
64. Kuntla, S.K. An Era of Sentinels in Flood Management: Potential of Sentinel-1, -2, and -3 Satellites for Effective Flood Management. *Open Geosci.* **2021**, *13*, 1616–1642. [CrossRef]
65. Tan, W.; Qin, N.; Zhang, Y.; McGrath, H.; Fortin, M.; Li, J. A Rapid High-Resolution Multi-Sensory Urban Flood Mapping Framework via DEM Upscaling. *Remote Sens. Environ.* **2024**, *301*, 113956. [CrossRef]
66. Klemas, V. Remote Sensing of Floods and Flood-Prone Areas: An Overview. *J. Coast. Res.* **2015**, *31*, 1005–1013. Available online: https://bioone.org/journals/journal-of-coastal-research/volume-31/issue-4/JCOASTRES-D-14-00160.1/Remote-Sensing-of-Floods-and-Flood-Prone-Areas{-}{-}An/10.2112/JCOASTRES-D-14-00160.1.full (accessed on 12 July 2025). [CrossRef]
67. Adjovu, G.E.; Stephen, H.; James, D.; Ahmad, S. Overview of the Application of Remote Sensing in Effective Monitoring of Water Quality Parameters. *Remote Sens.* **2023**, *15*, 1938. Available online: https://www.mdpi.com/2072-4292/15/7/1938 (accessed on 12 July 2025). [CrossRef]
68. NASA Earth Observatory. Devastating Floods in Pakistan. Available online: https://earthobservatory.nasa.gov/images/150279/devastating-floods-in-pakistan (accessed on 12 July 2025).
69. Gumbricht, T. Detecting Trends in Wetland Extent from MODIS Derived Soil Moisture Estimates. *Remote Sens.* **2018**, *10*, 611. Available online: https://www.mdpi.com/2072-4292/10/4/611 (accessed on 12 July 2025). [CrossRef]
70. Notti, D.; Giordan, D.; Caló, F.; Pepe, A.; Zucca, F.; Galve, J.P. Potential and Limitations of Open Satellite Data for Flood Mapping. *Remote Sens.* **2018**, *10*, 1673. Available online: https://www.mdpi.com/2072-4292/10/11/1673 (accessed on 12 July 2025). [CrossRef]
71. Amitrano, D.; Di Martino, G.; Di Simone, A.; Imperatore, P. Flood Detection with SAR: A Review of Techniques and Datasets. *Remote Sens.* **2024**, *16*, 656. Available online: https://www.mdpi.com/2072-4292/16/4/656 (accessed on 12 July 2025). [CrossRef]
72. Global Flood Awareness System—GloFAS News. Available online: https://global-flood.emergency.copernicus.eu/news/150-cems-global-flood-monitoring-annual-product-and-service-quality-assessment-report-2022/ (accessed on 11 July 2025).
73. Muhadi, N.A.; Abdullah, A.F.; Bejo, S.K.; Mahadi, M.R.; Mijic, A. The Use of LiDAR-Derived DEM in Flood Applications: A Review. *Remote Sens.* **2020**, *12*, 2308. Available online: https://www.mdpi.com/2072-4292/12/14/2308 (accessed on 12 July 2025). [CrossRef]

74. Tavus, B.; Kocaman, S.; Nefeslioğlu, H.; Gökçeoğlu, C. Flood Mapping Using Sentinel-1 SAR Data: A Case Study of Ordu 8 August 2018 Flood. *Int. J. Environ. Geoinf.* **2019**, *6*, 333–337. [CrossRef]
75. Planet Pulse. Copernicus EMS Uses Planet Data for Emergency Response Mapping. Available online: https://www.planet.com/pulse/copernicus-emergency-response-mapping/ (accessed on 12 July 2025).
76. Lakshmi, S.E.; Yarrakula, K. Review and Critical Analysis on Digital Elevation Models. *Geofizika* **2018**, *35*, 7–19. [CrossRef]
77. Betterle, A.; Salamon, P. Water Depth Estimate and Flood Extent Enhancement for Satellite-Based Inundation Maps. *Nat. Hazards Earth Syst. Sci.* **2024**, *24*, 2817–2836. [CrossRef]
78. Laefer, D.F.; O'Keeffe, E.; Chandna, K.; Hertz, K.; Zhu, J.; Lejano, R.; Vo, A.V.; Bertolotto, M.; Ofterdinger, U. Low-Cost, LiDAR-Based, Dynamic, Flood Risk Communication Viewer. *Remote Sens.* **2025**, *17*, 592. Available online: https://www.mdpi.com/2072-4292/17/4/592 (accessed on 12 July 2025). [CrossRef]
79. Wang, Z.; Zhang, C.; Atkinson, P.M. Combining SAR Images with Land Cover Products for Rapid Urban Flood Mapping. *Front. Environ. Sci.* **2022**, *10*, 973192. [CrossRef]
80. Cian, F.; Marconcini, M.; Ceccato, P. Flood depth estimation by means of high-resolution SAR and optical data: A Sentinel-based hybrid approach using Copernicus EMS reference layers. *Remote Sens. Environ.* **2024**, *308*, 114511. [CrossRef]
81. Cerri, M.; Steinhausen, M.; Kreibich, H.; Schröter, K. Are OpenStreetMap Building Data Useful for Flood Vulnerability Modelling? *Nat. Hazards Earth Syst. Sci.* **2021**, *21*, 643–662. [CrossRef]
82. Chen, S.; Liu, L.; Li, K.; Ding, X.; Jiang, W. Simulation and Prediction of the Expansion of OpenStreetMap Building Data Based on the Markov-FLUS Model in Shenzhen, China. *Taylor Fr. Online* **2025**, *40*, 2459109. Available online: https://www.tandfonline.com/doi/epdf/10.1080/10106049.2025.2459109?needAccess=true (accessed on 12 July 2025). [CrossRef]
83. Soliman, M.; Morsy, M.M.; Radwan, H.G. Assessment of Implementing Land Use/Land Cover LULC 2020-ESRI Global Maps in 2D Flood Modeling Application. *Water* **2022**, *14*, 3963. Available online: https://www.mdpi.com/2073-4441/14/23/3963 (accessed on 12 July 2025). [CrossRef]
84. Gemitzi, A.; Kopsidas, O.; Stefani, F.; Polymeros, A.; Bellos, V. A Constantly Updated Flood Hazard Assessment Tool Using Satellite-Based High-Resolution Land Cover Dataset Within Google Earth Engine. *Land* **2024**, *13*, 1929. Available online: https://www.mdpi.com/2073-445X/13/11/1929 (accessed on 12 July 2025). [CrossRef]
85. Lei, Y.; Cao, H.; Zhou, X.; Mills, J.; Xiao, W. Impact of Land Use/Land Cover Changes on Urban Flooding: A Case Study of the Greater Bay Area, China. *IEEE J. Sel. Top. Appl. Earth Obs. Remote Sens.* **2024**, *17*, 13261–13275. Available online: https://ieeexplore.ieee.org/document/10602531 (accessed on 12 July 2025). [CrossRef]
86. Psomiadis, E.; Diakakis, M.; Soulis, K.X. Combining SAR and Optical Earth Observation with Hydraulic Simulation for Flood Mapping and Impact Assessment. *Remote Sens.* **2020**, *12*, 3980. [CrossRef]
87. Qamer, F.M.; Abbas, S.; Ahmad, B.; Hussain, A.; Salman, A.; Muhammad, S.; Nawaz, M.; Shrestha, S.; Iqbal, B.; Thapa, S. A Framework for Multi-Sensor Satellite Data to Evaluate Crop Production Losses: The Case Study of 2022 Pakistan Floods. *Sci. Rep.* **2023**, *13*, 4240. [CrossRef]
88. Ajmar, A.; Boccardo, P.; Broglia, M.; Kucera, J.; Tonolo, F.G.; Wania, A. Response to Flood Events: The Role of Satellite-Based Emergency Mapping and the Experience of the Copernicus Emergency Management Service (EMS). In *Geophysical Monograph Series*; Wiley: Hoboken, NJ, USA, 2017; pp. 213–228. [CrossRef]
89. Long, S.; Fatoyinbo, T.E.; Policelli, F. Flood Extent Mapping for Namibia Using Change Detection and Thresholding with SAR. *Environ. Res. Lett.* **2014**, *9*, 035002. Available online: https://iopscience.iop.org/article/10.1088/1748-9326/9/3/035002/meta (accessed on 12 July 2025). [CrossRef]
90. Liu, B.; Li, Y.; Ma, M.; Mao, B. A Comprehensive Review of Machine Learning Approaches for Flood Depth Estimation. *Int. J. Disaster Risk Sci.* **2025**, *16*, 433–445. [CrossRef]
91. Panahi, M.; Jaafari, A.; Shirzadi, A.; Shahabi, H.; Rahmati, O.; Omidvar, E.; Lee, S.; Bui, D.T. Deep Learning Neural Networks for Spatially Explicit Prediction of Flash Flood Probability. *Geosci. Front.* **2021**, *12*, 101076. [CrossRef]
92. ResearchGate. Flood Detection in Sar Images Based on Multi-Depth Flood Detection Convolutional Neural Network. Available online: https://www.researchgate.net/publication/340300265_Flood_Detection_in_Sar_Images_Based_on_Multi-Depth_Flood_Detection_Convolutional_Neural_Network (accessed on 12 July 2025).
93. Hashi, A.O.; Abdirahman, A.A.; Elmi, M.A.; Mohd Hashi, S.Z.; Romo Rodriguez, O.E. A Real-Time Flood Detection System Based on Machine Learning Algorithms with Emphasis on Deep Learning. *Int. J. Eng. Trends Technol.* **2021**, *69*, 249–256. [CrossRef]
94. Notarangelo, N.; Wirion, C.; Winsen, F. STURM-Flood: A Curated Dataset for Deep Learning-Based Flood Extent Mapping Leveraging Sentinel-1 and Sentinel-2 Imagery. *Big Earth Data* **2025**, *16*, 1–27. [CrossRef]
95. Alonso-Sarria, F.; Valdivieso-Ros, C.; Molina-Pérez, G. Detecting Flooded Areas Using Sentinel-1 SAR Imagery. *Remote Sens.* **2025**, *17*, 1368. Available online: https://www.mdpi.com/2072-4292/17/8/1368 (accessed on 12 July 2025). [CrossRef]
96. May, F.; Cárdenas, O.; Toledo, G. Flood Mapping through Sentinel-1, Sentinel-2 Imagery and U-NET Deep Learning Model. *Comput. Sist.* **2025**, *29*, 5539. [CrossRef]

97. Fawakherji, M.; Blay, J.; Anokye, M.; Beni, L.H.; Dorton, J. DeepFlood for Inundated Vegetation High-Resolution Dataset for Accurate Flood Mapping and Segmentation. *Sci. Data* **2025**, *12*, 271. [CrossRef] [PubMed]
98. Mia, M.U.; Chowdhury, T.N.; Chakrabortty, R.; Pal, S.C.; Al-Sadoon, M.K.; Costache, R.; Islam, A.R. Flood Susceptibility Modeling Using an Advanced Deep Learning-Based Iterative Classifier Optimizer. *Land* **2023**, *12*, 810. Available online: https://www.mdpi.com/2073-445X/12/4/810 (accessed on 12 July 2025). [CrossRef]
99. ResearchGate. Can I Trust my Flood Maps? A Comprehensive Analysis of Validation Strategies. Available online: https://www.researchgate.net/publication/392986509_Can_I_Trust_my_Flood_Maps_A_Comprehensive_Analysis_of_Validation_Strategies (accessed on 12 July 2025).
100. ResearchGate. A Globally Sampled High-Resolution Hand-Labeled Validation Dataset for Evaluating Surface Water Extent Maps. Available online: https://www.researchgate.net/publication/373541802_A_globally_sampled_high-resolution_hand-labeled_validation_dataset_for_evaluating_surface_water_extent_maps (accessed on 12 July 2025).
101. UNOSAT. Available online: https://unosat.org/ (accessed on 12 July 2025).
102. EODC Public Wiki. echnical Overview of the GFM Product. Available online: https://extwiki.eodc.eu/GFM/PUM/TechnicalOverview (accessed on 12 July 2025).
103. FAO. Global Flood Monitoring-Annual Product and Service Quality Assessment Report 2022. Available online: https://www.fao.org/fishery/en/openasfa/fbc02883-5de2-4caf-807a-0b8c50ba45e8 (accessed on 12 July 2025).
104. Hajji, S.; Krimissa, S.; Abdelrahman, K.; Boudhar, A.; Elaloui, A.; Ismaili, M.; El Bouzekraoui, M.; Chikh Essbiti, M.; Kahal, A.Y.; Mondal, B.K.; et al. Enhancing Flood Prediction through Remote Sensing, Machine Learning, and Google Earth Engine. *Front. Water* **2025**, *7*, 1514047. [CrossRef]
105. Cohen, S.; Brakenridge, G.R.; Kettner, A.; Bates, B.; Nelson, J.; McDonald, R.; Huang, Y.F.; Munasinghe, D.; Zhang, J. Estimating Floodwater Depths from Flood Inundation Maps and Topography. *J. Am. Water Resour. Assoc.* **2018**, *54*, 847–858. [CrossRef]
106. Cohen, S.; Raney, A.; Munasinghe, D.; Loftis, J.D.; Molthan, A.; Bell, J.; Rogers, L.; Galantowicz, J.; Brakenridge, G.R.; Kettner, A.J.; et al. The Floodwater Depth Estimation Tool (FwDET v2.0) for Improved Remote Sensing Analysis of Coastal Flooding. *Nat. Hazards Earth Syst. Sci.* **2019**, *19*, 2053–2065. [CrossRef]
107. Peter, B.G.; Cohen, S.; Lucey, R.; Munasinghe, D.; Raney, A.; Brakenridge, G.R. Google Earth Engine Implementation of the Floodwater Depth Estimation Tool (FwDET-GEE) for Rapid and Large Scale Flood Analysis. *IEEE Geosci. Remote Sens. Lett.* **2022**, *19*, 1–5. [CrossRef]
108. Teng, J.; Penton, D.J.; Ticehurst, C.; Sengupta, A.; Freebairn, A.; Marvanek, S.; Vaze, J.; Gibbs, M.; Streeton, N.; Karim, F.; et al. A Comprehensive Assessment of Floodwater Depth Estimation Models in Semiarid Regions. *Water Resour. Res.* **2022**, *58*, e2022WR032031. [CrossRef]
109. Bryant, S.; McGrath, H.; Boudreault, M. Gridded Flood Depth Estimates from Satellite-Derived Inundations. *Nat. Hazards Earth Syst. Sci.* **2022**, *22*, 1437–1450. [CrossRef]
110. Poterek, Q.; Caretto, A.; Braun, R.; Clandillon, S.; Huber, C.; Ceccato, P. INterpolated FLOod Surface (INFLOS), a Rapid and Operational Tool to Estimate Flood Depths from Earth Observation Data for Emergency Management. *Remote Sens.* **2025**, *17*, 329. [CrossRef]
111. Copernicus EMS. Urban Flood INFLOS EXFLOS. Available online: https://emergency.copernicus.eu/documents/14/20241106_RM_ODW_Urban_Flood_INFLOS_EXFLOS.pdf (accessed on 11 July 2025).
112. Liou, Y.-A.; Hoang, D.-V. Improved Flood Depth Estimation with SAR Image, Digital Elevation Model, and Machine Learning Schemes. *J. Hydrol. Reg. Stud.* **2024**, *53*, 101775. [CrossRef]
113. Al-Aizari, A.R.; Alzahrani, H.; Althuwaynee, O.F.; Al-Masnay, Y.A.; Ullah, K.; Park, H.J.; Al-Areeq, N.M.; Rahman, M.; Hazaea, B.Y.; Liu, X. Uncertainty Reduction in Flood Susceptibility Mapping Using Random Forest and eXtreme Gradient Boosting Algorithms in Two Tropical Desert Cities, Shibam and Marib, Yemen. *Remote Sens.* **2024**, *16*, 336. [CrossRef]
114. Mobley, W.; Sebastian, A.; Blessing, R.; Highfield, W.E.; Stearns, L.; Brody, S.D. Quantification of Continuous Flood Hazard Using Random Forest Classification and Flood Insurance Claims at Large Spatial Scales: A Pilot Study in Southeast Texas. *Nat. Hazards Earth Syst. Sci.* **2021**, *21*, 807–822. [CrossRef]
115. Bentivoglio, R.; Isufi, E.; Jonkman, S.N.; Taormina, R. Deep Learning Methods for Flood Mapping: A Review of Existing Applications and Future Research Directions. *Hydrol. Earth Syst. Sci.* **2022**, *26*, 4345–4378. [CrossRef]
116. Lee, C.C.; Huang, L.; Antolini, F.; Garcia, M.; Juanb, A.; Brody, S.D.; Mostafavi, A. MaxFloodCast: Ensemble Machine Learning Model for Predicting Peak Inundation Depth and Decoding Influencing Features. *arXiv* **2023**, arXiv:2308.06228. [CrossRef]
117. Sasanapuri, S.K.; Dhanya, C.T.; Gosain, A.K. A Surrogate Machine Learning Model Using Random Forests for Real-Time Flood Inundation Simulations. *Environ. Model. Softw.* **2025**, *188*, 106439. [CrossRef]
118. Frame, J.M.; Nair, T.; Sunkara, V.; Popien, P.; Chakrabarti, S.; Anderson, T.; Leach, N.R.; Doyle, C.; Thomas, M.; Tellman, B. Rapid Inundation Mapping Using the US National Water Model, Satellite Observations, and a Convolutional Neural Network. *Geophys. Res. Lett.* **2024**, *51*, e2024GL109424. [CrossRef]

119. Tanim, A.H.; McRae, C.B.; Tavakol-Davani, H.; Goharian, E. Flood Detection in Urban Areas Using Satellite Imagery and Machine Learning. *Water* **2022**, *14*, 1140. [CrossRef]
120. Composto, R.W.; Tulbure, M.G.; Tiwari, V.; Gaines, M.D.; Caineta, J. Quantifying Urban Flood Extent Using Satellite Imagery and Machine Learning. *Nat. Hazards* **2025**, *121*, 175–199. [CrossRef]
121. Razavi Termeh, S.V.; Kornejady, A.; Pourghasemi, H.R.; Keesstra, S. Flood Susceptibility Mapping Using Novel Ensembles of Adaptive Neuro Fuzzy Inference System and Metaheuristic Algorithms. *Sci. Total Environ.* **2018**, *615*, 438–451. [CrossRef]
122. Chakrabortty, R.; Pal, S.C.; Janizadeh, S.; Santosh, M.; Roy, P.; Chowdhuri, I.; Saha, A. Impact of Climate Change on Future Flood Susceptibility: An Evaluation Based on Deep Learning Algorithms and GCM Model. *Water Resour. Manag.* **2021**, *35*, 4251–4274. [CrossRef]
123. Elkhrachy, I. Flash Flood Water Depth Estimation Using SAR Images, Digital Elevation Models, and Machine Learning Algorithms. *Remote Sens.* **2022**, *14*, 440. [CrossRef]
124. Khosravi, K.; Panahi, M.; Golkarian, A.; Keesstra, S.D.; Saco, P.M.; Bui, D.T.; Lee, S. Convolutional Neural Network Approach for Spatial Prediction of Flood Hazard at National Scale of Iran. *J. Hydrol.* **2020**, *591*, 125552. [CrossRef]
125. Fang, Z.; Wang, Y.; Peng, L.; Hong, H. Predicting Flood Susceptibility Using LSTM Neural Networks. *J. Hydrol.* **2021**, *594*, 125734. [CrossRef]
126. Popa, M.C.; Peptenatu, D.; Drăghici, C.C.; Diaconu, D.C. Flood Hazard Mapping Using the Flood and Flash-Flood Potential Index in the Buzău River Catchment, Romania. *Water* **2019**, *11*, 2116. [CrossRef]
127. Costache, R.; Ngo, P.T.T.; Bui, D.T. Novel Ensembles of Deep Learning Neural Network and Statistical Learning for Flash-Flood Susceptibility Mapping. *Water* **2020**, *12*, 1549. [CrossRef]
128. Wieland, M.; Martinis, S. A Modular Processing Chain for Automated Flood Monitoring from Multi-Spectral Satellite Data. *Remote Sens.* **2019**, *11*, 2330. [CrossRef]
129. Kao, I.-F.; Liou, J.-Y.; Lee, M.-H.; Chang, F.-J. Fusing Stacked Autoencoder and Long Short-Term Memory for Regional Multistep-Ahead Flood Inundation Forecasts. *J. Hydrol.* **2021**, *598*, 126371. [CrossRef]
130. Dong, S.; Yu, T.; Farahmand, H.; Mostafavi, A. A Hybrid Deep Learning Model for Predictive Flood Warning and Situation Awareness Using Channel Network Sensors Data. *Comput. Aided Civ. Eng.* **2021**, *36*, 402–420. [CrossRef]
131. Nogueira, K.; Fadel, S.G.; Dourado, Í.C.; Werneck, R.D.; Muñoz, J.A.; Penatti, O.A.; Calumby, R.T.; Li, L.T.; dos Santos, J.A.; Torres, R.D. Exploiting ConvNet Diversity for Flooding Identification. *IEEE Geosci. Remote Sens. Lett.* **2018**, *15*, 1446–1450. [CrossRef]
132. Kang, W.; Xiang, Y.; Wang, F.; Wan, L.; You, H. Flood Detection in Gaofen-3 SAR Images via Fully Convolutional Networks. *Sensors* **2018**, *18*, 2915. [CrossRef]
133. Sarker, C.; Mejias, L.; Maire, F.; Woodley, A. Flood Mapping with Convolutional Neural Networks Using Spatio-Contextual Pixel Information. *Remote Sens.* **2019**, *11*, 2331. [CrossRef]
134. Nemni, E.; Bullock, J.; Belabbes, S.; Bromley, L. Fully Convolutional Neural Network for Rapid Flood Segmentation in Synthetic Aperture Radar Imagery. *Remote Sens.* **2020**, *12*, 2532. [CrossRef]
135. Isikdogan, F.; Bovik, A.C.; Passalacqua, P. Surface Water Mapping by Deep Learning. *IEEE J. Sel. Top. Appl. Earth Obs. Remote Sens.* **2017**, *10*, 4909–4918. [CrossRef]
136. Zhao, G.; Pang, B.; Xu, Z.; Cui, L.; Wang, J.; Zuo, D.; Peng, D. Improving urban flood susceptibility mapping using transfer learning. *J. Hydrol.* **2021**, *602*, 126777. [CrossRef]
137. Gebrehiwot, A.; Hashemi-Beni, L. 3D Inundation Mapping: A Comparison Between Deep Learning Image Classification and Geomorphic Flood Index Approaches. *Front. Remote Sens.* **2022**, *3*, 868104. [CrossRef]
138. Ichim, L.; Popescu, D. Segmentation of Vegetation and Flood from Aerial Images Based on Decision Fusion of Neural Networks. *Remote Sens.* **2020**, *12*, 2490. Available online: https://www.mdpi.com/2072-4292/12/15/2490 (accessed on 3 July 2025). [CrossRef]
139. Hashemi-Beni, L.; Gebrehiwot, A.A. Flood Extent Mapping: An Integrated Method Using Deep Learning and Region Growing Using UAV Optical Data. *IEEE J. Sel. Top. Appl. Earth Obs. Remote Sens.* **2021**, *14*, 2127–2135. [CrossRef]
140. Hou, J.; Li, X.; Bai, G.; Wang, X.; Zhang, Z.; Yang, L.; Du, Y.E.; Ma, Y.; Fu, D.; Zhang, X. A deep learning technique based flood propagation experiment. *J. Flood Risk Manag.* **2021**, *14*, e12718. [CrossRef]
141. Guo, Z.; Leitao, J.P.; Simões, N.E.; Moosavi, V. Data-driven flood emulation: Speeding up urban flood predictions by deep convolutional neural networks. *J. Flood Risk Manag.* **2021**, *14*, e12684. [CrossRef]
142. Kabir, S.; Patidar, S.; Xia, X.; Liang, Q.; Neal, J.; Pender, G. A deep convolutional neural network model for rapid prediction of fluvial flood inundation. *J. Hydrol.* **2020**, *590*, 125481. [CrossRef]
143. Lei, X.; Chen, W.; Panahi, M.; Falah, F.; Rahmati, O.; Uuemaa, E.; Kalantari, Z.; Ferreira, C.S.; Rezaie, F.; Tiefenbacher, J.P.; et al. Urban flood modeling using deep-learning approaches in Seoul, South Korea. *J. Hydrol.* **2021**, *601*, 126684. [CrossRef]
144. Li, L.; Chen, Y.; Xu, T.; Liu, R.; Shi, K.; Huang, C. Super-resolution mapping of wetland inundation from remote sensing imagery based on integration of back-propagation neural network and genetic algorithm. *Remote Sens. Environ.* **2015**, *164*, 142–154. [CrossRef]

145. Li, L.; Chen, Y.; Xu, T.; Huang, C.; Liu, R.; Shi, K. Integration of Bayesian regulation back-propagation neural network and particle swarm optimization for enhancing sub-pixel mapping of flood inundation in river basins. *Remote Sens. Lett.* **2016**, *7*, 631–640. [CrossRef]
146. Chu, H.; Wu, W.; Wang, Q.J.; Nathan, R.; Wei, J. An ANN-based emulation modelling framework for flood inundation modelling: Application, challenges and future directions. *Environ. Model. Softw.* **2020**, *124*, 104587. [CrossRef]
147. Xu, Q.; Shi, Y.; Zhao, J.; Zhu, X.X. FloodCastBench: A Large-Scale Dataset and Foundation Models for Flood Modeling and Forecasting. *Sci. Data* **2025**, *12*, 431. [CrossRef] [PubMed]
148. Zanchetta, A.D.; Coulibaly, P. Probabilistic Forecasts of Flood Inundation Maps Using Surrogate Models. *Geosciences* **2022**, *12*, 426. [CrossRef]
149. Teng, J.; Jakeman, A.J.; Vaze, J.; Croke, B.F.W.; Dutta, D.; Kim, S. Flood inundation modelling: A review of methods, recent advances and uncertainty analysis. *Environ. Model. Softw.* **2017**, *90*, 201–216. [CrossRef]
150. Van de Sande, B.; Lansen, J.; Hoyng, C. Sensitivity of Coastal Flood Risk Assessments to Digital Elevation Models. *Water* **2012**, *4*, 568–579. [CrossRef]
151. Islam, T.; Zeleke, E.B.; Afroz, M.; Melesse, A.M. A Systematic Review of Urban Flood Susceptibility Mapping: Remote Sensing, Machine Learning, and Other Modeling Approaches. *Remote Sens.* **2025**, *17*, 524. [CrossRef]
152. Jafarzadegan, K.; Moradkhani, H.; Pappenberger, F.; Moftakhari, H.; Bates, P.D.; Abbaszadeh, P.; Marsooli, R.; Ferreira, C.; Cloke, H.L.; Ogden, F.; et al. Recent advances and new frontiers in riverine and coastal flood modeling. *Rev. Geophys.* **2023**, *61*, e2022RG000788. [CrossRef]